A minority of Th1 and Tfh effector cells express survival genes shared by memory cell progeny and require IL-7 or TCR signaling to persist.

A DISSERTATION
SUBMITTED TO THE FACULTY OF THE GRADUATE SCHOOL
OF THE UNIVERSITY OF MINNESOTA
BY

Kevin Charles Osum

IN PARTIAL FULFILLMENT OF THE REQUIREMENTS
FOR THE DEGREE OF
DOCTOR OF PHILOSOPHY

Marc K. Jenkins, Ph.D.

September 2024

Acknowledgements

I would like to thank my mentor Dr. Marc Jenkins for his guidance and support throughout my time in his lab. His guidance was crucial for the completion of this project and there is no doubt I am a better scientist because of his tutelage. I thank my thesis committee: Dr's. Brian Fife, David Masopust, Ingunn Stromnes and Kris Hogquist for all their insights and excellent advice. My colleagues in Marc Jenkins lab have also been indispensable for the completion of this thesis and they have my gratitude for their assistance.

Dedication

This work is dedicated to my entire family. Especially to my wife Sara Osum, my son Miles Osum, and my daughter Valerie Osum. You all have my eternal love.

Abstract

It is not clear how $CD4^+$ memory T cells are formed from a much larger pool of earlier effector cells. We found that transient systemic bacterial infection rapidly generates several antigen-specific Th1 and T follicular helper (Tfh) effector cell populations with different tissue residence behaviors. Each Th1 and Tfh effector cell type produced a similar memory cell type, which was maintained by IL-7, or in the case of germinal center Tfh cells, by the T cell antigen receptor (TCR). Although most cells of all varieties had transcriptomes indicative of cell stress and death at the peak of the response, some had already acquired a quiescence signature. This thesis demonstrates that acute infection induces differentiation of Th1 and Tfh effector cells, a minority of which quickly adopt a transcriptional program that allows escape from death and become memory cells that survive from sensing IL-7 or a TCR ligand.

Table of Contents

List of Figures

Page

Chapter 1

Chapter 3

Chapter 4

Chapter 5

Chapter 1 : Current understanding of T cell memory subsets and memory formation[1]

It has been known for millennia that people who get a certain infection rarely get that infection a second time [1]. This phenomenon, which we now refer to as immune memory, is caused by the proliferation of rare antigen-specific naïve B cells, $CD8^+$ T cells, and $CD4^+$ T cells that differentiate into microbe-killing effector cells, a fraction of which survive a contraction phase to become long-lived memory cells [2]. The increased abundance and anti-microbial functions of antigen-specific memory cells elicited by a particular infection increases the odds that their host will mount a rapid and protective immune response to subsequent episodes of that infection.

[1] Portions of this work have been previously published. Reprinted from: Osum KC, Jenkins MK. **Toward a general model of CD4+ T cell subset specification and memory cell formation**. Immunity. 2023 Mar 14;56(3):475-484. doi: 10.1016/j.immuni.2023.02.010. PMID: 36921574; PMCID: PMC10084496., Krueger PD, Osum KC, Jenkins MK. **CD4+ Memory T-Cell Formation during Type 1 Immune Responses**. Cold Spring Harb Perspect Biol. 2021 Dec 1;13(12):a038141. doi: 10.1101/cshperspect.a038141. PMID: 33903156; PMCID: PMC8635001.

During infection, naïve $CD4^+$ T cells with TCRs specific for MHCII-bound microbial peptides divide in secondary lymphoid organs and differentiate into Th1, Th2, or Th17 effector cells depending on type 1 (IL-12, type I IFN, IL-18), type 2 (IL-25, IL-33, TSLP, IL-4), or type 3 (IL-1, IL-6, TGF-β) cytokines, respectively, from cells of the innate immune system [4,5]. Th1, Th2, and Th17 cell differentiation is enforced by master transcription factors (T-bet, GATA-3, RORɣt) and associated with production of canonical lymphokines (IFN-γ, IL-4, and IL-17) that augment the microbicidal functions of myeloid cells and granulocytes [6]. In addition, some Th effector cells express the transcription factor, Bcl-6, and become T follicular helper (Tfh) cells that drive antibody affinity maturation by germinal center B cells [7]. Other variations on this theme have led to the appreciation of Th9 and Th22 cells and even less understood varieties such as Th3, T regulatory 1, and T peripheral helper cells [8–10]. Cells with the phenotypes of Th1, Th2, Th17, and Tfh cells can be found after the contraction phase and are thus presumably memory cells [11]. These memory T cells are further classified based on the expression of homing receptors and trafficking patterns. Central memory T cells (TCM) express lymph node homing receptors and recirculate through secondary lymphoid organs. Effector memory cells

(TEM) express homing receptors that facilitate recirculation through non-lymphoid tissue. Alternatively, resident memory cells reside in tissues for long periods of time without recirculating [12,13].

The wealth of information on Th subset specification has not been well integrated with the larger concepts of TCM, TEM, and TRM cells or cell-mediated and humoral immunity. Indeed, it seems possible that the many Th cell subsets and a focus on their differences has impeded our understanding of $CD4^+$ memory T cell formation. We aimed to understand how memory $CD4^+$ T cells form from their earlier effector phenotypes, define subsets that meet the requirements for the larger concept of TCM, TEM and TRM, and to understand the survival mechanisms that $CD4^+$ memory T cells use to persist for long periods of time.

T cell research based on MHC tetramers

Although Th cells can be studied with a variety of methods [14], this thesis has focused on direct ex vivo flow cytometric detection of epitope-specific CD4+ T cells with fluorophore-labeled peptide:MHCII tetramers [15,16] (Figure 1). This approach is powerful because it focuses unambiguously on T cells

that express TCRs specific for MHCII-bound peptides derived from the proteins of the microbe or vaccine of interest [17]. It avoids concerns about the physiological relevance of TCR transgenic T cells [18,19], in vitro culture artifacts, and bystander activation [20].

The precision afforded by peptide:MHCII tetramers allows high signal-to-noise quantification of natural Th cells over time [21] and gives information on the phenotype and function of the antigen-specific Th cell population as it transitions from the effector phase to the memory phase [22,23]. Although peptide:MHCII tetramers may miss some T cells with low affinity TCRs [15,24], this downside is offset by the high degree of confidence gained by knowing that tetramer-binding cells are truly specific for the antigen of interest.

The CD8+ memory T cell model

The power of the tetramer-based approach was demonstrated by Ahmed and colleagues, who used Lymphocytic Choriomeningitis Virus (LCMV) peptide:MHCI tetramers to show that many more post-infection $CD8^+$ T

cells were LCMV-specific than was previously thought [25]. This revelation established the tetramer-based approach as the bar for $CD8^+$ memory T cell research; a bar that could usually be cleared because peptide:MHCI tetramer-binding cells were abundant enough to detect during most intracellular infections. Indeed, the discovery of peptide:MHCI tetramers in 1996 [26] coincided with a surge in $CD8^+$ memory T cell research as evidenced by a Pubmed search with the terms “antigen-specific” AND “CD8 T cell” AND “memory” that shows a dramatic increase in publications beginning in 1997 and reaching a steady plateau of about 40 papers per year by 2006. Three years before this plateau, Kaech and Ahmed used a few cell surface markers to show that the LCMV epitope-specific $CD8^+$ effector T cell population is a mixture of 2 subsets: (1) memory cell precursors (MPEC) that express IL-7 receptor (IL-7R) and survive the contraction phase and (2) short-lived effector cells (SLEC) that lack IL-7R, express KLRG1, and are destined to die [27]. Although the resulting MPEC/SLEC theory was later modified from the knowledge that CD69, CX3CR1, CD103, and a few other markers could be used with IL-7R and KLRG1 to distinguish effector, central, resident, and peripheral memory cell subsets, and that some effector cells could be relatively long-lived [28], the

core model has persisted as a useful guide for the study of dozens of microbes, vaccines, and cancers. It is likely that this guiding theory of memory cell formation has attracted many immune memory-focused researchers to the $CD8^+$ T cell field.

Technical and biological challenges for CD4+ memory T cell researchers

The path to understanding $CD4^+$ memory T cell formation has lagged behind that of their $CD8^+$ counterparts. One likely reason is that less research has been done on this topic. A Pubmed search with the terms “antigen-specific” AND “CD4 T cell” AND “memory” yields only half as many publications from 1996 to date as the Comparable search with “antigen-specific” AND “CD8 T cell” AND “memory”. The reason for this disparity is not immediately obvious as it is clear from the deadly opportunistic infections that occur in individuals lacking $CD4^+$ T cells that this subset is worth studying [29].

Several factors likely play a part, not the least of which are technical. Single naïve $CD8^+$ T cells produce about 10,000 effector cells when their T cell

receptors (TCR) engage a peptide:MHCI agonist in the context of infection 30 whereas only 500 CD4+ effector T cells are detected from a single naïve cell under similar conditions [31]. The 10-fold difference in proliferation identified in these studies and others [32,33] makes it much easier to detect epitope-specific $CD8^+$ T cells than $CD4^+$ T cells. This technical advantage is especially valuable for the study of post-contraction phase memory T cells, which are 10–20-times less numerous than their effector cell predecessors. In many cases, peptide:MHCII tetramer-binding $CD4^+$ memory T cells can only be detected after labor intensive magnetic enrichment procedures [34]. Adding to the problem is the fact that peptide:MHCII tetramers are more difficult to produce than peptide:MHCI tetramers [35]. Many allelic forms of MHCII molecules must be produced in eukaryotic expression systems, which generally give lower yields than the bacterial systems. In addition, it is difficult to produce empty MHCII molecules that can be loaded with synthetic peptides without the action of HLA-DM or H-2DM, unlike MHCI molecules that can be refolded with synthetic peptides and beta-2 microglobulin [36]. Finally, MHCII-binding peptides are harder to predict than MHCI-binding peptides using algorithms [37] and the open ends of the peptide-binding grooves of MHCII molecules allow peptides to bind in more

than one register [16,38]. This makes it more difficult to identify new $CD4^+$ T cell epitopes – a necessary first step in peptide:MHCII tetramer production. It is easy to believe that this “death by a thousand technical nicks” has limited entry of new researchers into the $CD4^+$ memory T cell field.

Another barrier to progress in the $CD4^+$ memory T cell field has been the lack of a guiding model. The MPEC/SLEC model, which is so useful for the study of $CD8^+$ memory T cells, has been much less useful for $CD4^+$ T cells because epitope-specific $CD4^+$ effector T cell populations are often devoid of IL-7R+ and KLRG1+ cells [39], making it harder to identify MPECs and SLECs.

Finally, it is possible that one of the most interesting aspects of $CD4^+$ T biology – the plethora of Th cell subsets – has limited consensus building. The unique aspects of $CD4^+$ T cell differentiation during type 1, 2, and 3 immune responses and the seemingly endless parade of new subsets such as T regulatory 1, Th3, Th0, Th9, and Th22 cells may have captured the attention of researchers more than common features of all $CD4^+$ T cell responses or efforts to integrate the Th1/Th2 paradigm [40] with the TEM and TCM cell theory [13]. In summary, the technical difficulties related to detection

of epitope-specific Th cells and the huge effort needed to separately understand Th cell specification and trafficking may have been distractions from the creation of a model of Th memory cell formation.

A unifying function across Th subset diversity: synchronized support of cell-mediated and humoral immunity

Although there exists a diverse range of Th subsets, all $CD4^+$ T cell responses have a common feature of simultaneously supporting cell-mediated and humoral immunity. For example, while type 1, 2, and 3 immune responses involve macrophage-activating Th1, eosinophil-activating Th2, and neutrophil-activating Th17 cells, these responses also invoke IgG2a, IgE, and IgG3 production and Tfh-facilitated affinity maturation by B cells [41,42]. It is likely that simultaneous activation of phagocyte-activating and antibody-augmenting Th cells has evolved to provide a one-two punch for host immunity. The mechanism, however, that ensures the production of non-Th and Tfh cells in all types of immune responses is not totally clear, especially since as described below, these effector cell subsets form by mutually antagonistic pathways.

Identifying CD4+ effector and memory T cell subsets

Clues about how balanced immunity is achieved are emerging from studies of mouse $CD4^+$ memory T cell formation during type 1 immune responses to acute infections with LCMV [39,43–47], attenuated Listeria monocytogenes (aLm) bacteria [22,31], influenza A virus [48,49], or malaria parasites [50,51]. Work on these immune responses converges on a bifurcation model described below in which macrophage-helping Th1 and B cell-helping Tfh effector cells form simultaneously in secondary lymphoid organs and then a fraction of each type survive the contraction phase to become memory cells [11,51]. The model may have been slow to emerge, however, because of the use of different flow cytometry gating schemes for identifying effector and memory cell subsets. Some groups have relied on CXCR5 and PD-1 to distinguish Th1 and Tfh cells [22,46,52], while others have used Ly6C and P-selectin glycoprotein ligand 1(PSGL1), and in some cases folate receptor 4 (FR4) [39,47,53]. This dual track has persisted because each strategy has strengths and weaknesses but may have led to a focus on the “trees” rather than the “forest”.

The first approach has the advantage that CXCR5 is a known Tfh marker that is required for Tfh cells to migrate to follicles and germinal centers [54]. The simplest version of the strategy has the weakness, however, that Th1 cells are identified by lack of a marker - CXCR5. This problem is easily remedied by intracellular staining for T-bet [55] or surface staining for the Th1-associated chemokine receptor CXCR6 [44,51,56]. This approach identifies several epitope-specific populations during the effector phase - Th1 ($CXCR6^+$ $CXCR5^-$) and germinal center Tfh (GC-Tfh) ($CXCR6^-$ $CXCR5^{hi}$ $PD\text{-}1^+$) cells, and $CXCR6^-$ $CXCR5^{lo}$ cells 22,44 that are likely precursors of GC-Tfh cells[7,57] or GC-Tfh cells that migrated out of germinal centers[58] (Table 1). These cells will be referred to here as Tfh cells. There is another effector cell population that expresses the TCM marker CCR7[13]. The majority of these cells express CXCR5 [22,44,59], leading us to call them pre-TCM cells[22].

Counterparts of the effector cell subsets identified with this strategy are also found in the post-contraction memory cell population. Th1 ($CXCR5^-$) cells are detected along with a heterogenous $CXCR5^{lo}$ memory cell population that contains $CCR7^+$ and $CCR7^-$ subsets [22,44,59]. The inability of

this strategy to resolve the CCR7^{-} CXCR5^{lo} subset into Tfh- or GC-derived memory cells is a limitation. It is also not helpful that PD-1 and CCR7 staining, which are used to distinguish Tfh, GC-Tfh, and TCM cells usually do not result in baseline separation between populations and CXCR5 expression decreases as CXCR5^{+} effector cells become CXCR5^{+} memory cells[22].

The limitations of the CXCR5-based strategy have spurred the Ly6C/PSGL1-based approach. Although the functions of Ly6C and PSGL1 are not understood in this context, these molecules serve as valuable markers because they identify the same 3 subsets in both the effector and memory cell phases (Table 1). The Ly6C^{-} PSGL1^{-} population consists of GC-Tfh cells in the effector phase[39], and later, their memory cell progeny, which are the only memory cells that express large amounts of FR4[47]. The Ly6C^{+} PSGL1^{+} population[39,45] contains a subset of Th1 cells[60]. The limitation of this scheme lies with the Ly6C^{-} PSGL1^{+} population, which probably contains a mixture of CXCR5^{lo} CCR7^{+} pre-TCM or TCM, CXCR5^{lo} CCR7^{-} Tfh, and Ly6C^{-} Th1 cells[45,47].

By combining information from studies utilizing the two gating systems it is possible to deduce the existence of Ly6C^{-} CXCR6^{+} and Ly6C^{+} CXCR6^{+} Th1, CCR7^{-} CXCR5^{lo} PD-1^{-} FR4^{lo} Tfh, CCR7^{-} CXCR5^{hi} PD-1^{+} FR4intermediate GC-Tfh cells, and CCR7^{+} CXCR5^{lo} PD-1^{-} FR4^{lo} pre-TCM cells. Further support for these being different populations can be derived from single cell RNA sequencing experiments on LCMV peptide:MHCII tetramer-binding T cells. These data suggest that all Th1 cells express Cxcr6 but only some express Ly6c2, and that there are several populations that express Cxcr5 but differ with respect to expression of Sell (encodes CD62L) and Izumo1r (encodes FR4) (Andreatta et al., 2022; Ciucci et al., 2019; Khatun et al., 2020). Ly6C^{-} CXCR6^{+} and Ly6C^{+} CXCR6^{+} Th1 cells are detected after the contraction phase, as are populations that resemble Tfh effector cells but with less CXCR5, or GC-Tfh effector cells except with less CXCR5 and more FR4. A CCR7^{+} CXCR5^{lo} population is also detected at post-contraction times.

The phenotypic similarities between the Th effector and memory subsets suggests that about 10% of the cells in each of the effector cell subsets survives the contraction phase to become phenotypically similar but

quiescent memory cells as the infection is cleared[11,51]. In other words, 10% of Ly6C$^+$ Th1 effector cells become Ly6C$^+$ Th1 memory cells, 10% of GC-Tfh effector cells become GC-Tfh memory cells, and so on. Recent work from Shaw et al.[59] is consistent with this interpretation and shows that the transcription factor, Id3, is key to determining which Th1 and Tfh effector cells will become memory cells. Single cell RNA sequencing experiments support this model by identifying TCM, Th1, and Tfh memory cells that are transcriptionally related to TCM, Th1, and Tfh effector cells [61]. Direct assessment of this effector to memory cell transition concept, however, awaits experiments in which purified cells from the each of the effector cells subsets is transferred into infection-matched recipients and the phenotypes of their memory cell progeny are determined.

It is likely that each of the Th memory subsets plays a unique role during secondary immune responses. This hypothesis has been addressed experimentally by adoptive transfer of purified Th memory cell types from infected mice into naive recipients, immediately infecting the recipients with the initial microbe, and then assessing the phenotypes of the donor memory cell–derived effector cells. In the aLm model, we found that

purified CXCR5^{-} T-bet^{hi} memory cells generated a secondary effector cell population consisting of >95% CXCR5^{-} T-bet^{hi} cells 22. Ly6C expression by the transferred memory cells or their effector cell progeny was not measured in these experiments. In the LCMV model, several groups[45,47] showed that purified the Ly6C+ Th1 memory cells generated primarily Ly6C^{+} Th1 cells. Similar results were obtained in the herpes virus model system [60]. The secondary effector cell-generating potential of Ly6C^{-} Th1 memory cells has not been tested, although results from the aLm model showing that the total Th1 memory cell population only generated Th1 effector cells[22] indicates that Ly6C^{-} Th1 memory cells are committed to producing primarily Th1 effector cells during secondary responses. It should be noted, however, that the Id3+ subset of Th1 memory cells can generate some Tfh effector cells [59].

The situation is less clear for the CXCR5^{lo} Th memory cell subsets. We previously found that the total population of CXCR5^{lo} Th memory cells generated Th1, CXCR5^{lo}, and GC-Tfh effector cells after transfer into naive recipients then infected with aLm [22]. This result showed that the CXCR5^{+} Th memory cell population is more multipotent than the Th1 memory

population, which mainly produce Th1 effector cells. This approach, however, did not assess the potential of the individual TCM, Tfh, and GC-Tfh memory cell subsets, which later work showed were present in the transferred population[31,45]. Künzli et al. [47] addressed this issue by focusing on Ly6C$^-$ PSGL-1$^-$ FR4$^+$ memory cells, which probably consist mainly of GC-Tfh-derived memory cells. They found that these memory cells can generate some Th1 and Tfh effector cells and were the most efficient memory cell type at producing GC-Tfh effector cells during a secondary response. The true effector cell-generating potential of TCM and Ly6C$^-$ Th1 memory cells awaits an experiment in which these cells are studied in the absence of contributions from other memory cell subsets. The bulk of the evidence, however, is that Tfh- and GC-Tfh-derived memory cells and likely TCM cells are related subsets that can produce a wider variety of the effector cell types than Th1 memory cells.

In summary, the field is complicated by competing cell identification schemes and cataloging the true diversity of Th effector and memory cells induced by acute infections that drive type 1 innate immune responses. There is no doubt that these populations consist of a mixture of Th1 and

Tfh varieties. This thesis aims to find a consistent gating scheme that uncovers the total diversity of $CD4^+$ T cells and to understand how this mixture forms memory cells.

The bifurcation model

An emerging concept is that Th1 and Tfh subsets are formed by a process that will be referred to here as the bifurcation. The bifurcation is driven by an IL-2R signal-dependent switch, which we propose generates early non-Tfh and pro-Tfh cells that then differentiate into TCM, Th1, or Tfh cells effector cells based on cytokines from the innate immune system. Another feature of the model is that a fraction of the cells in each subset then survive the contraction phase to become memory cells that are phenotypically like their effector cell predecessors (Figure 2).

The earliest evidence for the bifurcation in the aLm model is observed the secondary lymphoid organs on day 3 after infection. The aLm epitope-specific $CD4^+$ T cell population has just begun to expand at this time and contains 2 main subsets – CD25 (IL-2 receptor (IL-2R) alpha chain)$^+$ cells that lack CXCR5 and $CXCR5^+$ cells that lack CD25[22]. This finding is

consistent with IL-2R signaling suppressing Tfh formation and promoting the generation of non-Tfh cells, which has been borne out in several studies [22,48,62]. The supposition is that some early effector cells within the mixed population receive signals from IL-2R and some that do not either because of lack of IL-2 production or IL-2R expression (Figure 1). The cells that receive IL-2R signals, activate STAT5 [63], which then activates BLIMPEC1, an inhibitor of Bcl-6 expression and Tfh formation [46,62,64]. Thus, the cells that receive STAT5 signals from the IL-2R cannot become Tfh cells and instead become non-Tfh cells. During type 1 immune responses, many of these non-Tfh cells become Th1 cells in response to STAT1 signals from type I and II IFN receptors, then STAT4 signals from IL-12 receptor [65–67]. Inflammatory monocytes play a key role in driving the non-Th cells to become Th1 cells [50,68]. The signals that determine whether Th1 cells express Ly6C are not known. It is likely, however, that Ly6C$^-$ Th1 cells are precursors of more differentiated Ly6C$^+$ Th1 cells although Ly6C$^+$ Th1 cells can revert to Ly6C$^-$ Th1 cells [60].

The other branch of the bifurcation occurs in cells that do not receive IL-2R signaling. These cells do not turn on BLIMPEC1 and thus are able to

express Bcl-6, which directs them toward the Tfh fate [46,69,70]. We propose that these early effector cells first become pro-Tfh cells and then Tfh cells if they receive STAT3 signals from IL-6 and IL-21 receptors 71. The Tfh cells then further differentiate into GC-Tfh cells if they receive signals from ICOS [22,72,73]. Bcl-6 induces this program by acting as a transcriptional repressor that shuts off the non-Tfh options [7,74] and by repressing repressors of the genes that positively regulate Tfh formation [75]. The transcription factors LEF1 and TCF-1 are involved in this process by sustaining expression of IL-6R and enhancing expression of ICOS [76–78]. Interestingly, the Tfh cells that form during the type 1 immune response to aLm express low amounts of T-bet[22] and malaria-induced Tfh cells produce IFN-ɣ [79], suggesting that Tfh cells adopt some features of their non-Th counterparts. This idea is supported by the existence of distinct human Tfh cells that express chemokine receptors that typify Th1, Th2, and Th17 cells [80–82] and presumably develop during type 1, 2, and 3 immune responses, respectively.

We also propose that during acute bacterial and viral infections, some early pro-Tfh cells do not receive signals from receptors for differentiating

cytokines, perhaps because of residence in niches in the secondary lymphoid organs lacking these molecules and retain the naïve T cell trafficking program dictated by CCR7 and other molecules. As the infection is cleared, we posit that these cells become TCM cells. It is possible, however, that some pathogens, such as Plasmodium (the causative agent of malaria), drive such large amounts of innate cytokines that all pro-Tfh cells are driven to become Tfh cells leaving very few to become TCM cells[51].

A key aspect of the bifurcation model is that non-Tfh and pro-Tfh cells form at the same time, and often in roughly equal amounts during acute infections [22,46]. Since a critical factor appears to be IL-2R signaling, it stands to reason that there is a mechanism that determines that some of the effector cells - the ones destined to become non-Tfh cells - get an IL-2R signal while the others do not. One possible origin of this heterogeneity is TCR-dependent induction of IL-2 and IL-2R, which are produced by naïve T cells in proportion to TCR signal strength[83]. Some naïve T cells may make more IL-2 and IL-2R due to expression of TCRs with high affinity for MHCII-bound peptides or chance engagement with antigen-presenting cells

displaying large amounts of peptide:MHCII complexes. In acute infections, intense IL-2R signaling favors induction of IRF4 and BLIMPEC1 over Bcl-6 [84–86], which would favor non-Tfh formation [84,87–89]. Other naïve T cells that have TCRs with lower affinity for the MHCII-bound peptide or happen to engage lower amounts of this ligand would be less likely to produce IL-2 or IL-2R and thus more likely to express Bcl-6 and become pro-Tfh cells. A twist on this idea is that some non-Tfh-fated effector cells may express the IL-2R but receive IL-2 from other cells [90]. Regulatory T (Treg) cells[91] and a subset of dendritic cells [92] play roles in this process by quenching IL-2 thereby favoring the production of pro-Tfh cells.

An attractive aspect of the bifurcation model is that it provides a mechanism for the simultaneous formation of Th cells that augment the microbicidal functions of granulocytes, myeloid, and epithelial cells, and other Th cells that help B cells make high affinity antibodies. It thus provides an explanation for the fact that the vast majority if not all adaptive immune responses to infection lead to both cell-mediated and T cell-dependent humoral immunity. Given the evolutionary advantage this two-pronged defense this system provides, it would make theoretical sense for

the bifurcation mechanism to be a general feature of all CD4+ T cell responses. Indeed, the simultaneous induction of Th2 cells and Tfh cells has been well documented in studies of type 2 immune responses [93–95]. As in type 1 immune responses, the non-Tfh cells, Th2 cells in this case, depend on IL-2R signals [94]. A surprising aspect of this story is that Tfh cells are better IL-4-producing cells than Th2 cells [94,95], which are potent producers of IL-5 and IL-13 and tend to migrate to non-lymphoid sites of infection [94]. Thus, certain infections induce Th2 cells, which are likely critical for IL-5-dependent activation of eosinophils at the site of infection, and Tfh cells, which probably produce the IL-4 needed to drive IgE switching by B cells.

There is also some evidence for the bifurcation in type 3 immune responses. Myelin peptide:MHCII-specific Th17 and Tfh cells can co-exist in mice with experimental autoimmune encephalomyelitis (EAE) [96]. In addition, Streptococcus pyogenes epitope-specific Th17 and Tfh cells form in nasal-associated lymphoid tissues of S. pyogenes-infected mice, and the Th17 cells are to some extent IL-2R-dependent[97]. It should be noted, however, that IL-2-deficient TCR transgenic $CD4^+$ T cells formed ***more***

Th17 cells than wild-type cells after adoptive transfer into wild-type recipients and priming with the relevant antigen in complete Freund's adjuvant [98]. This case is either an exception to the rule that IL-2R signaling is required for development of non-Tfh effector cells, or the IL-2-deficient T cells, which had the capacity to express IL-2R, received IL-2 from wild-type T cells in the adoptive recipient. The first possibility indicates that signals other than STAT5 may be able to drive BLIMPEC-1, suppress Bcl-6, and promote the Th17 fate in some contexts. Mechanism aside, studies of type 3 immune responses further suggest that simultaneous production of Tfh and non-Tfh effector cells is a core feature of all $CD4^+$ T cell responses that evolved to ensure that both humoral immunity and specialized forms of cell-mediated immunity occur at the same time.

Exceptions, opportunities, and challenges

There may be circumstances where one limb of the bifurcation becomes amplified over the other. The immune response to phagosomal pathogens is one case in point. These microbes, such as Mycobacterium tuberculosis and Salmonella enterica, establish persistent but $CD4^+$ T cell-controlled

infections of the phagolysosomes of myeloid cells [99]. Naïve $CD4^+$ T cells with TCRs specific for MHCII-bound peptides from these microbes proliferate and form an early effector cell population consisting of Th1 and Tfh cells as predicted by the bifurcation model [49]. As infection proceeds, however, the Th1 cells proliferate more than the Tfh cells such that Th1 cells account for the vast majority of the population several weeks into the infection. At this point, the Th1 population develops two subsets also observed following M. tuberculosis infection [100], one expressing CXCR3 and capable for more IFN-γ production than the Th1 cells that form during acute infections and a subset that expresses markers of terminal differentiation such as KLRG1 or CX3CR1 [49,101]. In M. tuberculosis infection, the $CXCR3^+$ cells express PD-1 and remarkably are dependent on Bcl-6 to form efficiently even though the cells are Th1 cells[102]. They also provide superior protection again M. tuberculosis infection[100,102]. These results suggest that although the bifurcated production of Th1 and Tfh cells is the first response of the system, certain conditions such as persistent intracellular bacterial infection in an IL-12-rich environment can cause the prolonged proliferation and further differentiation of Th1 cells.

It is conceivable that other conditions, perhaps microenvironments lacking IL-2, will favor the Tfh limb. Indeed, chronic LCMV infection, which induces T cell exhaustion and loss of IL-2 production[103], leads to accumulation of Tfh-like cells[104]. This idea may also be worth considering for immune responses that occur under non-inflammatory conditions. Indeed, we found the bifurcation model helpful when interpreting results from experiments on the $CD4^+$ T cell response to food antigens. We previously showed that a food peptide:MHCII-specific Th population generated by antigen feeding contained 3 major subsets – Treg cells, TCM-like cells, and GC-Tfh-like cells[105]. Although the TCM-like and GC-Tfh-like cells lacked CXCR5 and were hyporesponsive to antigenic stimulation, single cell RNA sequencing revealed that that they share many markers with the TCM and GC-Tfh cells that form during infections. In addition, the Treg cell population formed in an IL-2-dependent fashion. It is therefore possible that this response is a variation of the bifurcation process that occurs under IL-2 limited conditions with most cells not receiving IL-2R signals and entering the Tfh path but failing to become genuine Tfh cells due to a lack of IL-6 and IL-21 and progressive unresponsiveness due to chronic TCR signaling. The few cells

that engage IL-2 under these conditions may adopt the non-Tfh fate and in this case become peripheral Treg cells.

Although the cases in the preceding 2 paragraphs are essentially corollaries to the bifurcation rule, more direct challenges for the theory lie ahead. More basic research must be done in mice to assess whether the bifurcation model truly applies to type 3 immune responses. There is also a need to determine whether signals in addition to those from the IL-2R contribute to the formation of non-Tfh cells. Although IL-2R-deficiency greatly reduces Th1 cell formation it is not completely eliminated in the way that Bcl-6-deficiency completely wipes out all the $CXCR5^+$ subsets[22].

It also seems important to determine the roles that Th memory cell subsets play in protective immunity. This work will require relevant infection models and will likely have model-specific features, which will complicate and yet enrich the search for consensus. The utility of Th1 memory cells producing IFN-γ and stimulating myeloid cells to kill intracellular bacteria is easy to appreciate. But even in this case, the relative protective capacities and mechanisms of the 4 known Th1 subsets - $Ly6C^-$ and $Ly6C^+$ Th1 cells from acute infections [60] and $CXCR3^+$ and $CX3CR1^+$ Th1 cells from controlled

persistent phagosomal infections [100,101] – are not completely understood. In addition, it is possible that different Th1 subsets disinfect different myeloid cell types, for example some focusing on monocytes, others on macrophages, or in different anatomic locations.

The protective function of GC-Tfh-derived memory cells is very likely to provide GC-Tfh effector cells to drive further affinity maturation of the germinal center cell progeny of memory B cells during subsequent infections[7]. Research from the HIV field indicates that many rounds of this process must occur to produce the rare antibodies that can neutralize many different HIV variants and are thus the goal of current vaccine strategies[106]. It should be noted, however, that TCM, Tfh, and GC-Tfh-derived memory cells can generate some Th1 effector cells during secondary responses [22,39,45,47]. It is not known whether the Th1 effector cells generated from these memory cells are different from those derived from Th1 memory cells.

More research is also needed to integrate information about Th1, Th2, Th17, and Tfh differentiation into the cell trafficking-based TCM and TEM theory of Sallusto and Lanzavecchia[13], and later modifications to account

for TRM cells[12]. The recirculation properties of the Ly6C$^-$ Th1 memory cells, however, are unknown and we hypothesized that that these could be TEM cells. Along this line, it was of interest to determine whether GC-Tfh effector cells, which are likely resident in secondary or tertiary lymphoid organs, give rise to GC-Tfh, Tfh, or TCM, the great majority of CCR7$^+$ memory cells also express CXCR5 [22,59] and are related to Tfh cells based on disappearance in Bcl-6 deficient mice [22]. It should be pointed out, however, that although the human TCM population defined by the CD45RA$^-$ CXCR7$^+$ phenotype contains a prominent CXCR5+ subset, it also contains CXCR5$^-$ cells, some of which express the Th1 marker CXCR3[107]. This fact points to the existence of conditions that generate TCM cells that are related to Th1 cells instead of Tfh cells. Perhaps the CD62L$^+$ CXCR5$^-$ Th memory cells described by Hale et al. [45] are these cells. Another wrinkle is that the LCMV-induced mouse Th1 population, which lacks the TCM marker, CCR7, still contains a subset that has the TCM gene expression signature [59]. These issues need to be sorted out to gain a better understanding of the CD4$^+$ TCM population. The Ly6C$^+$ Th1 cells fit the definition of TEM cells as they can be found in secondary lymphoid organs and non-lymphoid tissues[89] and have been shown to recirculate through these sites [108]. The

answers to these questions would close the gap in research on $CD4^+$ TRM cells, which is lagging behind that on $CD8^+$ TRM cells[12].

The bifurcation model also needs vetting in humans. This will be a difficult task because early aspects of the bifurcation process occur in secondary lymphoid organs that are hard to access in people. Although epitope-specific Th1 and Tfh cells have been detected in the peripheral blood of humans [81], the full spectrum of Th cell phenotypes in people is only beginning to be understood. Unfortunately, the myriad flow cytometry gating schemes used to characterize human $CD4^+$ T cells will again complicate progress in this area. A scheme that could be used across species would be a boon to the $CD4^+$ memory T cell field. In addition, the extensive polymorphism of MHCII molecules in the human population[113] will continue to be a barrier to MHCII tetramer-based approaches to the study of human $CD4^+$ memory T cells. The $CD8^+$ T cell field has dealt with MHCI polymorphism by focusing peptide:MHCI tetramer-based studies on a common MHCI allelomorph - HLA-A2 114. The fact that HLA-DP4 is expressed by up to 60% of people[115] offers a similar opportunity to the

$CD4^+$ T cell field although many HLA-DP4-restricted peptides will have to be discovered.

In summary, this thesis answers some of the proposed questions we believe would advance our understanding of CD4 memory formation and is based on the bifurcation model as a conceptual framework to guide our experiments about memory T cell research. This framework and the conclusions we show here, could help the field come to a consensus about $CD4^+$ memory T cell formation and survival amid the torrent of single cell RNA sequencing data that offers the temptation of further subdividing similar subsets from different infections.

Statement of thesis

My thesis is that after differentiation each subset of $CD4^+$ T cells has the capacity to form memory cells that are similar to their effector counterparts and that memory cells either rely on Il7r signaling, IL7r/IL15 signaling or TCR stimulation to survive.

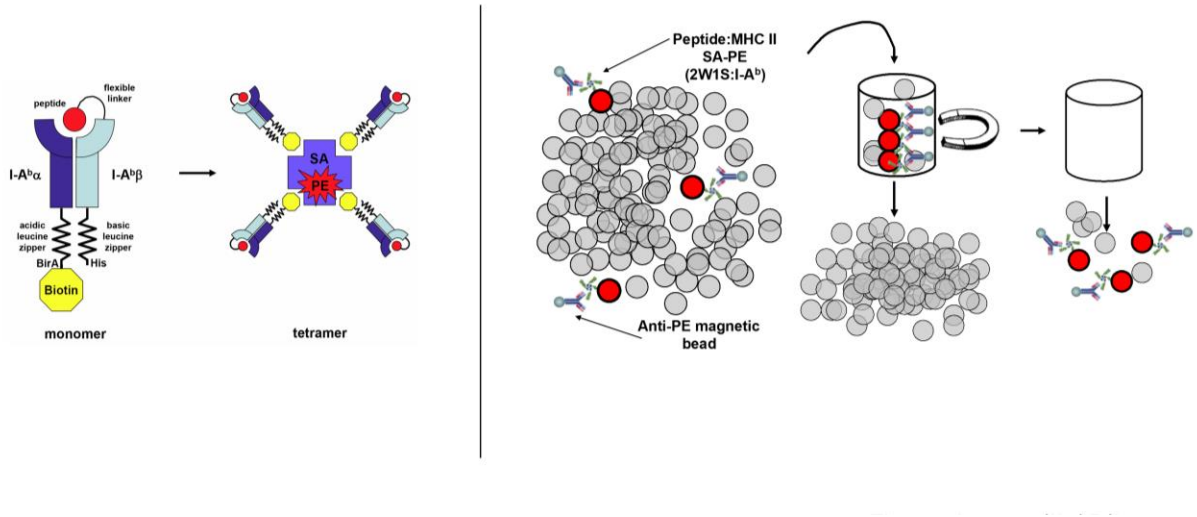

Diagram 1. Visual description of Tetramer enrichment technology

I-A^b monomers are tetramerized to streptavidin APC or PE by the tetramers biotin tail. Staining a single cell suspension with I-A^b tetramers allows for labelling of rare antigen specific cells and are then labelled with an anti-PE or APC antibody that is conjugated to a magnetic bead. Passing the labelled mixture through a magnet results in the retention of the tetramer labelled cells in the magnetic column. The column is then eluted and run on a flow cytometer for further analysis.

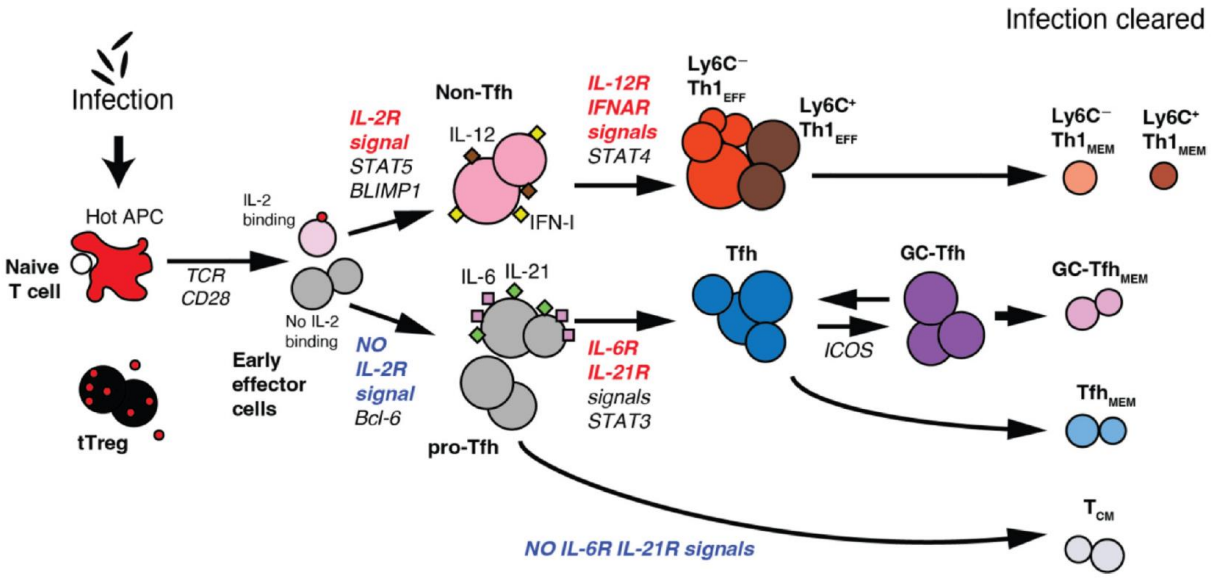

Model 1. Model of CD4$^+$ T cell bifurcation and memory formation

Naïve CD4+ T cells interact with antigen bearing antigen presenting cells and undergo expansion into early effector cells that audition for Th1 or Tfh differentiation. In the presence of IL-2 early effector cells differentiate into Th1 cells that can either be Ly6C- or Ly6C+. When IL-2 is limiting the cells differentiate into Tfh and can migrate to the B cell zone. Some cells will receive further signals to enter the B cell zone and become GC-Tfh where they can provide B cell help. The cells that do not receive signals from a B cell reside in the mantle zone area where they are termed Tfh. Some Tfh will form memory cells of the same phenotype and some may upregulate CCR7 or CD62L to become T central memory cells.

Table 1.
Markers used to identify Th effector and memory cell subsets by flow cytometry.

The symbols indicate a range of protein expression levels from negative (−) to various degrees of positivity from + to ++++. Values are based on the literature and our unpublished data.

	CD62L	CXCR6	Ly6C	FR4	PSGL1	CXCR5
Effector cells						
Pro-Tfh	++++	−	−	++	++	++
$Ly6C^{+}$ $Th1_{EFF}$	−	++++	++++	+	++++	−
$Ly6C^{-}$ $Th1_{EFF}$	−	+++	−	−	++++	−
Tfh_{EFF}	−	−	−	+++	++	+++
GC-Tfh_{EFF}	−	−	−	+++	−	++++
Memory cells						
TCM	++++	−	−	++	++	+
$Ly6C^{+}$ $Th1_{MEM}$	−	++++	++++	−	++++	−
$Ly6C^{-}$ $Th1_{MEM}$	−	++++	−	−	++++	−
Tfh_{MEM}	−	−	−	++	++	+
GC-Tfh_{MEM}	−	−	−	++++	−	+

Table 1. Expression levels of different Th1 effector and memory population for the makers given above.

Chapter 2 : Methods and materials

Mice

Female C57BL/6 (B6), B6.SJL-Ptprca Pep3b/BoyJ (CD45.1+), B6.129S6-Tbx21tm1Glm/J (*Tbx21 -/-*)90, B6(Cg)-Il15tm1.2Nsl/J (*Il15 -/-*)91, (B6.129S(FVB)-Bcl6tm1.1Dent/J (*Bcl6 fl/fl*)92, B6.Cg-Tg(Lck-icre)3779Nik/J (*Lck Cre/Cre*)93, B6.Cg-Ndor1Tg(UBC-cre/ERT2)1Ejb/1J (*Ubc Cre-ERT2*)94, and B6(129X1)-Tg(Cd4-cre/ERT2)11Gnri/J (*Cd4 Cre-ERT2*)95 mice were purchased from The Jackson Laboratory. *Bcl6fl/fl* mice were bred with *Lck Cre/Cre* mice to generate *Lck Cre/WT Bcl6 fl/fl* and *Lck WT//WT Bcl6 fl/fl* mice. *Il7r fl/fl* mice[96] were obtained from Alfred Singer and crossed to *Cd4 Cre-ERT2/WT* mice to produce *Cd4 Cre-ERT2/WT Il7r fl/fl* and *Cd4 WT/WT Il7r fl/fl* mice.

Parabiotic Surgeries

Parabiotic surgery was performed as described.[97] Briefly, mice to be joined were anesthetized and their sides to joined were shaved from about 1 cm below the shoulder and about 1 cm above the hip. Matching skin incisions were made in the shaved areas and with 3-0 Prolene stitches and overlying surgical wound clips. Parabionts were then allowed to rest for 21 days

before experiments. Percent residence was calculated as follows: percent resident = (1-(number of cells of a Th subset from the joined mouse x 2)/(number of cells of that subset from the joined mouse + number of cells of that subset from the parent mouse) x 100)). The number of cells of a Th subset from the joined mouse and the parent mouse for a joined pair were normalized to the number of 2W:IA^{b} tetramer− naive CD4^{+} T cells from the joined mouse and the parent mouse with the assumption that naive CD4^{+} T cells should distribute equally to each member of the pair. For example, consider a pair of joined day 30 CD45.1^{+} and CD45.2^{+} aLm-2W infected mice. The CD45.2 partner has 142 CD45.1^{+} tetramer^{+} M-Tfh cells, [53] CD45.2^{+} tetramer^{+} M-Tfh cells, 547 tetramer^{-} naive CD45.1^{+} T cells and 1,403 tetramer− naive CD45.2^{+} T cells. The CD45.1^{+} tetramer^{+} M-Tfh cells would be corrected to 253 (142 x ((547 + 1403)/2)/547)). The CD45.2^{+} tetramer^{+} M-Tfh cells would be corrected to 126 (182 x ((547 + 1403)/2)/1403)). These values were then entered into the formula described above.

Single-cell RNA sequencing

2W:I-A^{b} and LLOp:I-A^{b} tetramer-binding T cells were purified by FACS sorting from the SLOs of 6-10 mice per group infected intravenously 6, 21, or 60 days earlier with[107] aLm-2W bacteria. Cells from each sample loaded into one port of a 10X Genomics chip at 1,500 cells/μl. Libraries were prepared for each sample and sequenced using a Novaseq S4 chip (2 × 150-bp PE) at the University of Illinois. Features were enumerated using Cellranger (version 3.0, 10X Genomics) and gene expression values were analyzed using Seurat 5.0.0.98 Single cells from each sample were identified based on hashtags and normalized within each pool using the sctransform method in Seurat. Different clusters were visualized using UMAP dimensional reduction.[35]

Cell transfer

For the experiments shown in Figure 3, 2W:I-A^{b} and LLOp:I-A^{b} tetramer-binding cells were enriched from the spleen and lymph nodes of CD45.1^{+} mice 7 days after aLm-2W infection using Miltenyi positive selection kits according to the manufacturer's instructions. The cells were stained with phenotyping antibodies, purified by sorting on a FACSAria-II (BD) flow

cytometer based on gates shown in Figure 3A, and injected intravenously into separate mice expressed a different congenic marker, and had been infected 7 days earlier with aLm-2W bacteria. 2W:I-A^b tetramer-binding cells were enriched from the spleen and lymph nodes of the recipient mice 21 days later, stained with phenotyping antibodies, and analyzed for the various memory cell subsets as in Figure 2A.

Infections and injections

The ActA-deficient aLm-2W bacterial strain was described previously.[14] Mice were injected intravenously with 107 bacteria. For the experiments in Figure 6D, mice were infected with aLm-2W bacteria and then 40 days later, twice intraperitoneally with 1 mg of YTS177 CD4 antibody (Bio-X-Cell) or control IgG, 7 days apart. Subsets of 2W:I-A^b and LLOp:I-A^b tetramer-binding memory cells were analyzed 11 days after the second antibody injection.

Tetramers

Biotin-labeled I-A^b molecules containing the 2W (EAWGALANWAVDSA) or LLOp (NEKYAQAYPNVS) peptides covalently attached to the I-Ab beta chain were produced with I-A^b alpha chains in Drosophila melanogaster S2 cells[16,19,99,] then purified and tetramerized with streptavidin allophycocyanin (APC) as described previously.[16]

Cell enrichment and flow cytometry

Livers were perfused with Dulbecco's PBS via the portal vein until they changed color. Intrahepatic lymphocytes were isolated by gentleMACS (Miltenyi) disruption using the liver 01.01 program and incubated for 30 minutes at 37°C with shaking in 0.4 mg/ml collagenase IV and 25 µg/ml DNAse I. Single cell suspensions were spun at 300 rpm for 3 minutes to remove hepatocytes. Lymphocytes were purified on a 21% Histodenz gradient after centrifugation at 2,200 rpm for 20 minutes without braking and slow acceleration at 27oC. Single cell suspensions of pooled spleens and lymph nodes or liver preparations were stained for one hour at room temperature with APC-conjugated peptide:I-A^b tetramers[17] and BV650- or PE- conjugated CXCR5 antibodies and BV421- or BV711-conjugated

CXCR6 antibodies. Cells were enriched using the EasySep Mouse APC Positive Selection (STEMCELL Technologies) or Miltenyi Biotec systems according to the manufacturer's instructions. Enriched samples were stained for 20 minutes at 4°C with GhostDye Red 780 and fluorophore-conjugated antibodies specific for: CD4, B220, CD11b, CD11c, F4/80, CD44, CXCR5, PD-1, PSGL1, CD62L, CXCR6, and Ly-6C and in some cases CD45.2 and CD45.1. Stained cells were fixed and permeabilized with the FOXP3/Transcription Factor Staining Buffer Set (TONBO) according to the manufacturer's instructions and stained overnight at 4°C with fluorophore-conjugated Foxp3 and T-bet antibodies. Cells were counted and analyzed by flow cytometry with counting beads on a Fortessa (BD) flow cytometer. Data were analyzed using FlowJo software.

Immunofluorescence

Harvested murine tissues were embedded in OCT and frozen in a 2-methyl butane liquid bath. Seven-micron sections were cut on a Leica cryostat and stained with fluorophore-conjugated antibodies specific for BV421 CD19 (BD, 1D3), APC IgD (biolegend, 11-26c.2a), PE Thy1.2 (eBioscience, 53-

2.1), or FITC GL7 (biolegend, GL7). Whole spleen sections were tiled for GC quantitation using a Leica Thunder microscope and 20x 0.5 NA objective. Two sections 100 microns apart were stained and averaged for the number of GC's and follicles. High resolution images of GCs were acquired with a Leica Stellaris 8 confocal microscope. GC regions were tiled using 20x 0.75NA and 40x motCORR 1.25NA glycerol immersion objectives with xy voxel sizes of 0.568um and 0.284um, respectively. Captured images were analyzed using Imaris 8 software. Background fluorescence differences between images were equalized.

Chapter 3: Phenotype and location of CD4 T cell responses to aLm-2W[2]

Introduction

$CD4^+$ memory T cells play critical roles in immune protection to intracellular pathogens.[118] Memory cells are formed during infection from a process that begins when naive $CD4^+$ T cells with microbial peptide:MHCII-specific T cell receptors (TCR) proliferate and differentiate into effector cells that help clear the pathogen.[11] Although ninety percent of the effector T cells die by apoptosis during the contraction phase after the pathogen is eliminated, the remaining cells survive to become long-lived memory cells[33,121]. The leading paradigm for how memory cells are formed is based on observations of $CD8^+$ T cells. The pool of $CD8^+$ effector T cells contains both IL-7 receptor $(IL\text{-}7R)^+$ memory precursor cells (MPECs) that are destined to survive the contraction phase, and transcriptionally distinct[122], $IL\text{-}7R^-$ short-lived effector cells (SLECs) that are destined to die[27]. This model, however, may not apply to $CD4^+$ T cells as evidenced by the fact that adoptively transferred $IL\text{-}7R^+$ and $IL\text{-}7R^-$ CD4+ effector cells produce memory cells

equally well[39]. Thus, the mechanism by which $CD4^+$ memory T cells emerge from a larger pool of effector cells is not known. Understanding $CD4^+$ memory T cell formation has been complicated by the plethora of CD4+ T cell subsets. Naive $CD4^+$ T cells can differentiate into Th1, Th2, Th9, Th17, Th22, peripheral regulatory T (Treg) cell, or T follicular helper (Tfh) cells[125], and each of these cell types may have memory cell versions[11]. $CD4^+$ memory T cells can also exist as central (TCM), effector (TEM), or resident (TRM) cell varieties that recirculate through secondary lymphoid organs (SLOs), non-lymphoid organs, or reside permanently in tissues[126,127.] $CD4^+$ memory T cells also have complex survival requirements with the homeostatic cytokines IL-7 and IL-15 playing dominant but complex roles[33, 121–130]. It is unclear if $CD4^+$ T effector cell subsets are equally capable of forming memory cells, and if so, whether $CD4^+$ T cell memory formation conforms to the MPEC/SLEC paradigm of $CD8^+$ T cells. Here, we address these knowledge gaps using a type 1 immune response to acute bacterial infection in mice as a model system. Using peptide:MHCII tetramers, we identified several Th1 and Tfh cell populations that each yielded a phenotypically similar memory cell subset. The memory cell subsets had different trafficking patterns and variable

dependence on IL-7, IL-15, or TCR signaling, but expressed a similar set of genes regulating survival. Although most cells in the preceding effector cell population had transcriptomes indicative of cell stress and death, some had already acquired the memory cell gene signature. The results demonstrate that acute infection induces rapid differentiation of Th1 and Tfh effector cells, a minority of which quickly adopt a transcriptional program that allows them to survive the contraction phase and become memory cells while retaining their Th1 or Tfh identity.

RESULTS

The primary $CD4^+$ T cell response has expansion, contraction, and memory phases. We used a transient bacterial infection that induces type 1 immunity to study $CD4^+$ memory T cell formation. Mice were infected with an attenuated strain of *Listeria monocytes* (aLm)[131] engineered to express an immunogenic peptide, 2W1S, which binds to the I-A^b MHCII molecule and is recognized by about 300 naive T cells per uninfected C57BL/6 (B6) mouse[21]. We used a fluorophore-conjugated 2W:I-A^b tetramer-based cell enrichment method and flow cytometry[34] to identify when and where

memory cells are formed. 2W:I-A^b tetramer-binding $CD4^+$ T cells (Figure 1) underwent rapid proliferation after intravenous aLm-2W infection, peaking in the SLOs on days 5-7 at about 200,000 cells and then falling to 20,000 cells by day 15 (Figure 1A). The expanded population was dominated by $Foxp3^-$ conventional T cells and contained very few $Foxp3^+$ regulatory T (Treg) as observed in another type 1 immune response[135]. 2W:I-A^b tetramer-binding $CD4^+$ T cells also peaked in the liver and blood at 20,000 and 10,000 cells, respectively, on days 5-7, and then fell 10-fold by day 15 (Figure 1A). The number of cells in each location did not change significantly between days 15 and 30 although other work showed a slow numerical decline of memory cells after day 30 of acute infection[22,23,39]. These results suggest that the peak of effector T cell generation occurs after intravenous aLm-2W infection around day 6 and is followed by a contraction phase in all sampled body sites that ends around day 15 after which memory cells emerge. As noted below, the transcriptomes of aLm-induced $CD4^+$ cells did not change between days 21 and 60. Therefore, day 21 aLm-induced $CD4^+$ T cells are suitable for analysis of the memory state.

aLm-2W infection drives formation of many effector cell varieties.

Previous research showed that aLm infection induces a mixture of Th1 and Tfh effector and memory cells[22,39,45,46,139–141]. We used a flow cytometry strategy described by Marshall et al.[39] based on Ly-6C[143], a member of the Ly-6 superfamily, and P-selectin glycoprotein [127] (PSGL1), a receptor for P-selectin, and added the Tfh marker CXCR5[22,46,72] , the Th1-associated marker CXCR6[44,58], and the TCM marker CD62L[126,127] to identify as many previously described effector and memory cell types as possible.

Effector cells were characterized by analysis of 2W:I-A^b tetramer-binding conventional $CD4^+$ T cells in mice infected 7 days earlier with aLm-2W bacteria. As described for Lymphocytic Choriomeningitis Virus (LCMV)-specific $CD4^+$ T cells[39,45,47], the 2W:I-A^b tetramer-binding conventional $CD4^+$ T cell populations in aLm-2W-infected mice consisted of Ly-$6C^{hi}$ $PSGL1^+$, Ly-$6C^{lo}$ $PSGL1^+$, and Ly-$6C^-$ $PSGL1^-$ varieties (F. 1B). The Ly-$6C^{hi}$ $PSGL1^+$ cells expressed CXCR6 and the Th1 master transcription factor T-bet[146] but lacked CD62L and CXCR5 (Figure 1C). These cells were Th1 cells because they were absent in aLm-2W-infected mice lacking the *Tbx21* gene encoding T-bet (Figure 1D). The Ly-$6C^-$ $PSGL1^-$ cells expressed the

largest amounts of CXCR5 and PD-1, less T-bet than the Ly-6C^{hi} Th1 cells and lacked CXCR6 and CD62L (Figure 1C). These cells were greatly reduced in aLm-2W-infected mice lacking the *Bcl6* gene in T cells (Figure 1E), which established their identify as Tfh cells. Expression of relatively large amounts of PD-1 marked these cells as germinal center Tfh (GC-Tfh) cells[147].The Ly-6C^{lo} PSGL1^{+} population contained CXCR6^{+} CD62L^{-}, CXCR6^{-} CD62L^{+}, and CXCR6^{-} CD62L^{-} subsets (Figure 1B). The CXCR6^{+} CD62L^{-} cells lacked CXCR5 and expressed the same amount of T-bet as the Ly-6C^{hi} Th1 cells (Figure 1C) but experienced only a small and not statistically significant reduction T-bet-deficient mice (Figure 1D). As described below, however, these cells are transcriptionally very similar to the Ly-6C^{hi} Th1 cells and will be referred to as Ly-6C^{lo} Th1 cells for this reason. The 2 Ly-6C^{lo} PSGL1^{+} CXCR6^{-} populations expressed CXCR5, less T-bet than the Th1 cells and less PD-1 than the GC-Tfh cells (Figure 1C). The CXCR6^{-} CD62L^{-} cells were Tfh cells as evidenced by reduction in aLm-2W-infected mice with T cell specific deletion of the *Bcl6* gene (Figure 1E). This population was also reduced in Tbet- deficient mice (Figure 1D), although this could have been an indirect effect of loss of Ly-6C^{hi} Th1 cells. The lower level of PD-1 expression (Figure 1C) indicated that the CXCR6^{-}

CD62L^{-} cells were likely the follicular mantle zone Tfh (M-Tfh) cells identified in imaging studies[147]. Surprisingly, the CXCR6^{-} CD62L^{+} cells formed normally in the absence of Bcl-6 (Figure 1E) but lacked CXCR5 in this case (Figure 1F). Therefore, although CXCR5 expression in this population is controlled by Bcl-6, these cells do not require Bcl-6 to form. These cells, which resemble a subset identified by Feng et al.[148] will be referred to as pre-Tfh cells based on cell transfer experiments described below. Together, these results indicate that acute systemic bacterial infection induces Ly-6C^{hi} Th1, Ly-6C^{lo} Th1, pre-Tfh, M-Tfh, and GC-Tfh effector cells.

We then assessed the heterogeneity of the 2W:I-A^{b} tetramer-binding memory cell population that survived after the contraction phase days 21 after aLm-2W infection to determine if any of the effector cell subsets were not represented as a memory cell population. The subset composition of the day 21 population, however, was remarkably like that of the day 7 population. Ly-6C^{hi} PSGL1^{+}, Ly-6C^{lo} PSGL1^{+}, and Ly-6C^{-} PSGL1^{-} varieties were present and the Ly-6C^{hi} PSGL1^{+} cells expressed CXCR6 and T-bet but lacked CD62L and CXCR5 (Figures 2A and 2B). The Ly-6C^{-} PSGL1^{-}

cells again expressed CXCR5 and PD-1, less T-bet than the PSGL1^{+} Th1 cells and lacked CXCR6 and CD62L. The Ly-6C^{lo} PSGL1^{+} population again contained CXCR6^{+} CD62L^{-}, CXCR6^{-} CD62L^{+}, and CXCR6^{-} CD62L^{-} varieties and the CXCR6^{+} CD62L^{-} cells lacked CXCR5 and expressed the same amount of T-bet as the Ly-6C^{hi} Th1 cells. The Ly- C^{lo} PSGL1^{+} CXCR6^{-} CD62L^{-} and CD62L^{+} populations expressed CXCR5 but less than at day 7, less T-bet than the Th1 cells, and lacked PD-1. Thus, the post-contraction 2W:IA^{b} tetramer-binding memory T cell population contained varieties that resembled the Ly-6C^{hi} Th1, Ly-6C^{lo} Th1, pre-Tfh, M-Tfh, and GC-Tfh effector cells present on day 7. Indeed, the percentages of cells with these phenotypes were nearly identical at days 7 and 21 indicating that each subset underwent the same amount of contraction (Figure 2C). Cells with the phenotypes of Ly-6C^{hi} Th1, Ly-6C^{lo} Th1, pre-Tfh, and M-Tfh, subsets were also present in the blood on days 7 and 21 after aLm-2W infection, whereas GC-Tfh cells were difficult to detect in this location. The only significant change in the blood over time was that Ly-6Clo Th1 cells accounted for a smaller fraction of the day 21 than the day 7 population, consistent with progressive residency in tissues. 2W:I-A^{b} tetramer binding cells also migrated to the liver, a tissue with Lm tropism[149], and the

population was dominated by Ly-6C^{hi} Th1 and Ly-6C^{lo} Th1 cells at both days 7 and 21. Thus, the phenotype and localization of memory cell subsets were like the earlier effector cells subsets. No effector cell subsets were missing from the memory pool, suggesting that none were comprised exclusively of SLECs. The low representation of Ly-6C^{lo} Th1 and GC-Tfh memory cells in the blood suggested that these cells resided in tissues longer than the other memory cell types.

We performed a parabiosis experiment to test this possibility. Mice with different congenic markers were infected with aLm-2W bacteria and surgically joined 60 days later such that their blood supplies were shared[150]. CD4$^+$ T cells that bound 2W:I-A^b tetramer or an I-A^b-tetramer containing a peptide (LLOp) from the listeriolysin O protein that is naturally expressed by Lm[151] were analyzed to increase the number of aLm specific cells in the experiment. Tetramer-binding CD4$^+$ memory T cells from each parabiont were assessed 21 days after joining to allow time for recirculating populations to reach equilibrium. The Ly-6C^{hi} Th1, M-Tfh, and pre-Tfh memory cell populations moved between the SLOs of the parabionts, whereas Ly-6C^{lo} Th1 and GC-Tfh memory cells were more likely to remain

in the parabiont in which they were generated (Figure 2D). These results and those from the blood and liver (Figure 2C) indicate that M-Tfh and pre-Tfh cells are TCM cells that recirculate through SLOs (Figure 2C), whereas Ly-6C^{hi} Th1 cells are TEM cells that recirculate through SLOs and liver. Ly-6C^{lo} Th1 and GC-Tfh memory cells are SLO TRM cells and Ly-6C^{lo} Th1 cells may also reside in the liver.

Memory cell populations are derived from similar effector cell populations.

The results raised the possibility that the memory cell populations were each derived from the corresponding effector cell population, rather than a unique MPEC cell population. We tested this possibility by using an adoptive transfer approach. 2W:I-A^{b} and LLOp:IA^{b} tetramer-enriched Ly-6C^{hi} Th1, Ly-6C^{lo} Th1, pre-Tfh, M-Tfh, and GC-Tfh effector cells were sorted from the SLOs of day 7 aLm-2W-infected mice (Figure 3A). The purity of the post-sort Ly-6C^{hi} Th1, Ly-6C^{lo} Th1, M-Tfh, and GC-Tfh populations was greater than 95 percent and the pre-Tfh population was greater than 85 percent (Figure 3B). The sorted cells were injected intravenously into mice expressing a different congenic marker, which had

been infected 7 days earlier with aLm-2W bacteria. The phenotypes of the transferred 2W:I-A^b tetramer-binding T cells were then determined 3 weeks later after the effector-to-memory cell transition occurred. Ly-$6C^{hi}$ Th1 effector cells mainly produced Ly-$6C^{hi}$ and Ly-$6C^{lo}$ Th1 and some M-Tfh memory cells (Figures 3C and 3D). Ly-$6C^{lo}$ Th1 effector cells produced mostly Ly-$6C^{lo}$ Th1 and some M-Tfh memory cells. M-Tfh effector cells mainly produced mainly M-Tfh and some Ly-$6C^{lo}$ Th1 memory cells, whereas GC-Tfh effector cells mainly produced GC-Tfh and M-Tfh memory cells. The pre-Tfh effector cell donor population, which consisted of about 90% pre-Tfh and 10% M-Tfh cells at the time of transfer, generated a memory cell population of 25% pre-Tfh and 40% M-Tfh memory cells with smaller populations of Ly-$6C^{lo}$ Th1 and GC-Tfh memory cells. Thus, Ly-$6C^{hi}$ Th1, Ly-$6C^{lo}$ Th1, pre-Tfh, M-Tfh, and GC-Tfh effector cells each produced memory cells with the matching phenotype. Each effector cell type, especially pre-Tfh cells, however, also had some capacity to produce other memory cell types.

Discussion

Tracking the many phenotypes of $CD4^+$ effector and memory cells has posed a challenge due to subsets lacking specific markers, moreover some of the markers change over the course of the infection. An example of this is the Tfh marker CXCR5. While highly expressed on effector cells, Tfh downregulate this receptor as the infection clears making it challenging to track this population over time. We used the markers PSGL1, Ly6C, CXCR6 and CD62L to describe five subsets of effector and memory cells. The non-Tfh lineages, identified by persistence in the absence of the Tfh master transcription factor BCL6, were comprised of $CD62L^+$ pre-Tfh, $Ly6C^{hi}$ Th1, and $Ly6C^{lo}$ Th1 cells. $CD62L^+$ cells are likely the earliest pre-bifurcation population that may give rise to Th1 and Tfh. $CD62L^+$ cells meet the definition of Tcm although their presence at the peak of infection might better fit the nomenclature Tcmp described by Ciucci et al.[44] $CD62L^+$ effector cells largely gave rise to themselves and to pre-Tfh after the contraction. This could be due to CD62L shedding or to further differentiation into pre-Tfh from remaining antigen in the host. The $Ly6C^{lo}$ Th1 cells were the most surprising subset as they do not rely on the Th1

master transcription factor Tbet but they have high levels of Tbet expression. The Ly6C^{lo} Th1 were one of two resident populations that we were able to detect. Tbet independent interferon gamma producing cells are not well defined in the literature but they would likely have the novel characteristics that we have described here. Identifying this population as CXCR6^{+} and Ly6C^{lo} may help other areas of immunology track this resident Th1 like population in other infections and locations. The Ly6C^{hi} Th1 population has been well characterized in the literature and are bona fide Th1 with Tem like properties. The RNAseq, shown later in this thesis, suggests this population is likely a more mature Th1 population that gives rise to the CX3CR1^{+} which are a terminally differentiated Th1 population that dominates virulent phagosomal infections. The Ly6C^{hi} Th1 effector cells gave rise to Ly6C^{hi} and Ly6C^{lo} Th1 populations suggesting the acquisition of a resident memory Th1 population may be flexible through the contraction of Th1 cells.

The two populations of BCL6 dependent cells were PSGL-1^{hi} M-Tfh and PSGL1^{lo} GC-Tfh. The M-Tfh population largely generated memory versions

of themselves, shared CXCR5 expression with the GC-Tfh population, and recirculated through conjoined mice the same as Naïve cells. This population was absent from the liver which ruled out a designation of TEM, rather they appear to be TCM. The conventional marker assigned to TCM is CCR7 or CD62L. It's possible that these cells express CCR7[22] but not CD62L but the fact cells exhibiting this mixed phenotype can recirculate to the same extent as naïve cells caution the use of a single marker to identify cells with a recirculation pattern of canonically described Tcm. The GC-Tfh population was the second resident population that we identified by the lack of PSGL1 expression. This method of identification remained stable over time which is the main benefit over using CXCR5 and PD-1. It is unclear what role PSGL1 could be playing in residency due to $Ly6C^{lo}$ Th1 expression of this marker but also exhibit a resident like phenotype.

We demonstrated a flow cytometry panel capable of identifying five populations of effector and memory $CD4^+$ T cells in response to an acute bacterial infection and that each population prefers to form memory cells that are the same phenotype as the effector cells. Further, we describe the

trafficking patterns that each population uses to surveil the host at a memory timepoint. The identification of a novel Th1 and Tfh resident population may provide insight into different ways that T cells can remain resident within SLO's. Each subset forming a similar memory subset by the cell transfer approach did not align with the MPEC/SLEC model that has been illuminating for $CD8^+$ T cell research but it did not address what transcriptional changes occurred between the peak of the response and the resulting memory populations.

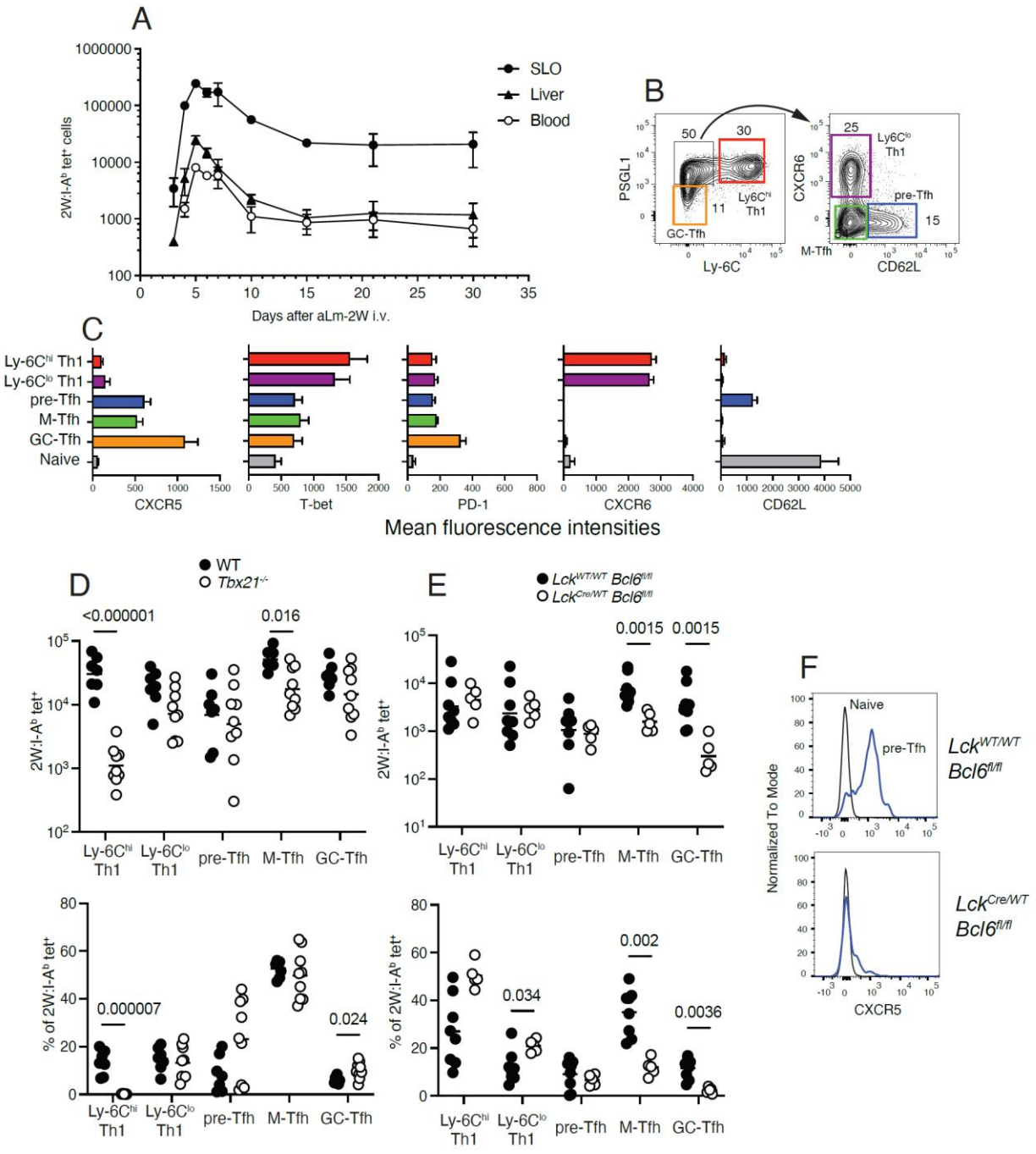
A
2W:I-Ab tet+ cells
Days after aLm-2W i.v.
SLO
Liver
Blood
B
PSGL1
Ly-6C
50
30
11
GC-Tfh
Ly6Chi Th1
CXCR6
CD62L
25
Ly6Clo Th1
pre-Tfh
15
M-Tfh
C
Ly-6Chi Th1
Ly-6Clo Th1
pre-Tfh
M-Tfh
GC-Tfh
Naive
CXCR5
T-bet
PD-1
CXCR6
CD62L
Mean fluorescence intensities
D
WT
Tbx21-/-
<0.000001
0.016
2W:I-Ab tet+
% of 2W:I-Ab tet+
0.000007
0.024
Ly-6Chi Th1
Ly-6Clo Th1
pre-Tfh
M-Tfh
GC-Tfh
E
LckWT/WT Bcl6fl/fl
LckCre/WT Bcl6fl/fl
0.0015
0.0015
0.002
0.034
0.0036
F
Naive
pre-Tfh
Normalized To Mode
LckWT/WT Bcl6fl/fl
LckCre/WT Bcl6fl/fl
CXCR5

Figure 1. Naive 2W:I-Ab-specific T cells undergo expansion after intravenous infection with aLm-2W bacteria. Memory cell populations are phenotypically like effector cell populations.

(A) Mean numbers (±}SD) of 2W:I-Ab tetramer-binding cells in the indicated organs of B6 mice (n ≥ three at each time point from two independent experiments) at the indicated times after aLm-2W infection. (B) Flow cytometry plots of staining of the indicated proteins on 2W:I-Ab tetramer+ cells from the SLOs of mice, 7 days after aLm-2W infection. (C) Mean fluorescence intensities of antibody staining of the indicated proteins on the indicated subsets identified as in (B). (D) Numbers (top) and percentages (bottom) of 2W:I-Ab tetramer-binding cells of the indicated subsets from the SLOs of individual WT (filled circles) or *Tbx21 -/-* (open circles) mice (n ≥ six from two independent experiments) on day 7 after aLm-2W infection. Mean values are indicated with a horizontal bar. (E) Numbers (top) and percentages (bottom) of 2W:I-Ab tetramer-binding cells of the indicated subsets from the SLOs of individual *Lck WT/WT Bcl6 fl/fl* (filled circles) or *Lck Cre/WT Bcl6 fl/fl* (open circles) mice (n ≥ five from two independent experiments) on day 7 after aLm-2W infection. Mean values are indicated

with a horizontal bar. (F) Histograms of CXCR5 staining on 2W:I-A^b tetramer-binding pre-Tfh cells (blue) or naive 2W:I-A^b tetramer− $CD4^+$ T cells (black) from mice of the indicated genotypes on day 7 after aLm-2W infection.

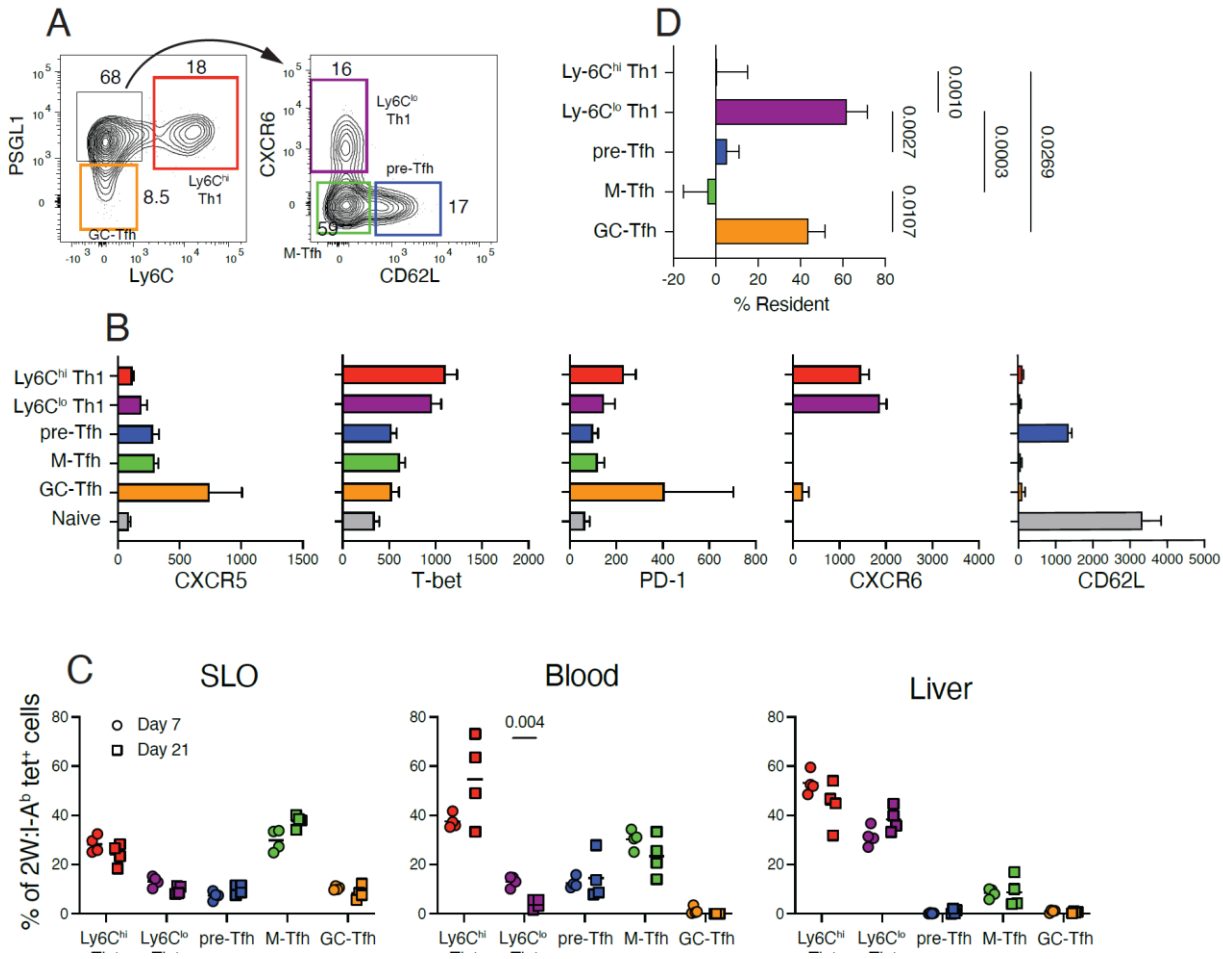

Figure 2. Phenotype and location of 2W:I-Ab-specific memory T cells after intravenous infection with aLm-2W bacteria.

(A) Flow cytometry plots of staining of the indicated molecules on 2W:I-A^b tetramer+ cells from the SLOs of mice, 21 days after aLm-2W infection. (B) Mean fluorescence intensities of antibody staining of the indicated proteins on the indicated subsets identified as in (A). (C) Percentages of 2W:I-A^b

tetramer-binding cells of the indicated subsets from the SLOs, blood, or livers of mice (n = 4 from two experiments) on day 7 (circles) or day 21 (squares) after aLm-2W infection. Mean values are indicated with a horizontal bar. The only significant difference between day 7 and 21 for a subset is shown with an adjusted P value from a Multiple unpaired T test. (D) Mean percentages (± SD, n 9-10 from 3 independent experiments) of the indicated 2W:I-A^b tetramer-binding memory cell subsets that did not recirculate between the SLOs of the parabionts in a 21-day period (% Resident). P values were derived from a oneway ANOVA with a Tukey's multiple comparisons test. One outlying value was removed from the $Ly6C^{hi}$ Th1 cell group based on the ROUT method with a Q value of 1%.

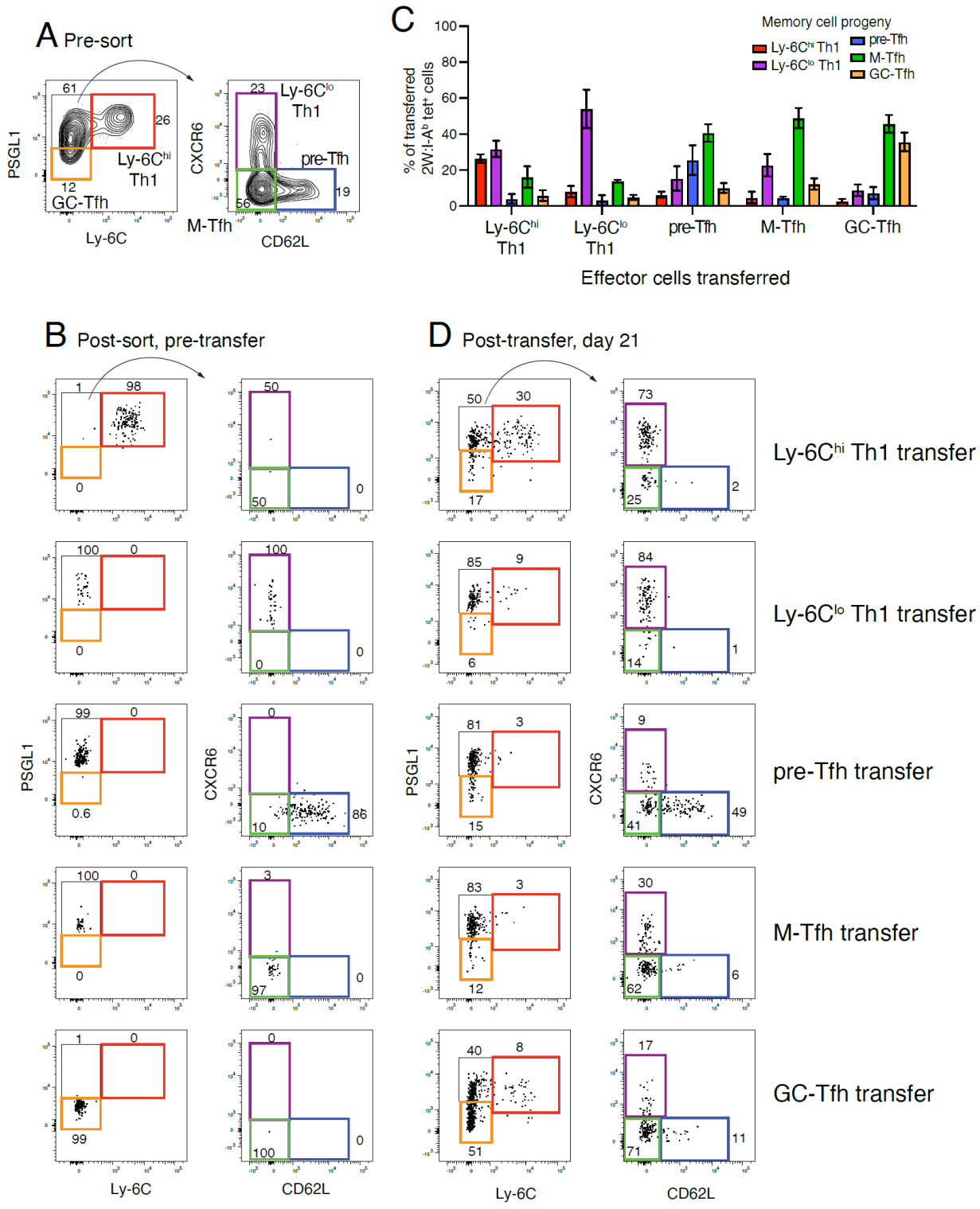
A Pre-sort
PSGL1
Ly-6C
61
26
12
Ly-6C^hi Th1
GC-Tfh
CXCR6
CD62L
23
Ly-6C^lo Th1
pre-Tfh
19
56
M-Tfh
C
% of transferred 2W:I-A^b tet+ cells
Memory cell progeny
Ly-6C^hi Th1
Ly-6C^lo Th1
pre-Tfh
M-Tfh
GC-Tfh
Ly-6C^hi Th1
Ly-6C^lo Th1
pre-Tfh
M-Tfh
GC-Tfh
Effector cells transferred
B Post-sort, pre-transfer
D Post-transfer, day 21
Ly-6C^hi Th1 transfer
Ly-6C^lo Th1 transfer
pre-Tfh transfer
M-Tfh transfer
GC-Tfh transfer
Ly-6C
CD62L

Figure 3. CD4+ effector T cell subsets generate phenotypically similar memory T cell subsets.

(A) Flow cytometry plots of the indicated molecules on 2W:I-A^b tetramer+ cells from the SLOs of CD45.2+ mice, 7 days after aLm-2W infection from a sample later subjected to FACS sorting. (B) Flow cytometry plots of the indicated molecules on 2W:I-A^b tetramer+ effector cells of the indicated subsets from SLOs of day 7 aLm-2W-infected CD45.2+ mice after FACS sorting based on the gates shown in (A). (C) Mean percentages (±} SEM, n ≥ 3 from 4 independent experiments) of 2W:I-A^b tetramer-binding memory cell subsets of CD45.2+ donor origin in CD45.1+ mice that received the indicated FACS-sorted CD45.2+ effector cell populations 21 days earlier. (D) Flow cytometry plots of the indicated molecules on 2W:I-A^b tetramer+ memory cells derived from the indicated FACS-sorted effector cell subsets 21 days after transfer into day 7 aLm-2W-infected recipients.

Chapter 4. Single cell RNA sequencing reveals transcriptionally distinct Th1 and Tfh effector cells.

An unbiased single cell transcriptomics study was then performed to identify potential mechanisms governing the effector-to-memory cell transition. 2W:I-A^b and LLOp:I-A^b tetramer-binding cells were enriched and sorted from SLOs on days 6, 21, or 60 after aLm-2W infection and single cells were subjected to an RNA sequencing protocol. Using the Seurat R package, the sequencing data from all time points (11,000 cells from day 6, 5,000 from day 21 and 5,000 from day 60) were integrated before quality control assessment and a Uniform Manifold Approximation and Projection (UMAP) plot was generated containing cells clustered by transcriptional state[152]. The effector to memory cell transition was readily apparent based on the segregation of cells along the X-axis of the UMAP plot (umap_1). Greater than 96 percent of the cells from day 6 had negative umap_1 values, whereas greater than 95 percent of the cells from day 21 or 60 had positive umap_1 values (Figure 4A). 10 percent of the day 6 cells had umap_1 values less than -5 (umap_1low) and expressed *Mki67* indicative of cell cycle progression[153]. Eighty-seven percent of the day 6 cells,

however, did not express *Mki67* and had intermediate umap_1 values between -5 and 0 (umap_1int), while 4 percent were *Mki67* – and had umap_1 values greater than 0 (umap_1high) like the memory cell populations present on days 21 and 60. We then identified a module of 19 differentially expressed genes (DEGs) with at least 2.5-fold higher expression in the day 6 versus the day 21 population. The effector module was filtered to exclude genes expressed by less than 10 percent of the day 6 cells or genes with highly variable expression along the Y-axis (umap_2). We similarly generated a DEGs list of 20 genes whose expression was enriched in memory cells. The effector cell module contained genes involved in apoptosis (*Gsn*, *S100a11*, *Lxn*, *Klf10*, *Gstt2*, *Casp3*, *Pycard, Rilpl2*) in different contexts[154–161], inhibition of T cell activation (*Pdcd1*, *Tigit*)[162,163], or $CD8^+$ effector T cell activation (*Irf4*, *Irf8*, *Ctla2b*)[164–166]. (Table 2), whereas the memory module contained genes involved in cell survival (*Bcl2*, *Prkce, Scml4, Pde2*)50–53, transcriptional repression (*Atn1*, *Nr1d2*)[171,172], vesicular trafficking (*Vps37b*, *Rab6b*)[173,174], or cGMPEC-mediated signaling (*Pde2a*, *Rundc3b*)[49,175] (Table 3). As expected, the effector module was expressed more by the day 6 than the 21 and day 60 populations (Figure 4B), whereas the memory module was expressed more

by the day 21 and day 60 populations than the day 6 population (Figure 4C). Importantly, however, the day 6 umap_1high cells showed low expression of the effector module (Figure 4B) and high expression of the memory module (Figure 4C). Likewise, umap_1int cells with higher umap_1 values were enriched for the memory module over the effector module (Figure 4B). Thus, although most of the cells in the day 6 population had an effector cell transcriptome associated in part with cell death, a minority already had the memory cell transcriptome.

While umap_1 segregated cells with effector or memory phenotypes, umap_2 segregated cells by T helper phenotype. At all times, the cells with umap_2 values greater than 0 expressed a module of Th1 genes including *Tbx21* (encoding T-bet), *Ifng*, *Nkg7*, and *Ccl5* (Figure 4D), whereas the cells with umap_2 values less than 0 expressed a module of Tfh genes including *Cxcr5, Il6st, Il6ra,* and *Btla* (Figure 4E). The effector (day 6) and memory (days 21 and 60) time points contained a similar fraction of cells expressing either the Th1 or Tfh module. This pattern was also observed among the day 6 cells already expressing the memory module (umap_1hi and umap1int cells with the highest umap_1 values). Thus, a minority of

Th1 and Tfh cells with memory cell transcriptomes are present as early as day 6 among a larger population of cells with effector cell transcriptomes. Notably, the umap_1low *Mki67*$^{+}$ cycling cells on day 6 (Figs. 4A) expressed the Th1 module but not the Tfh module (Figure 4D), consistent with the work of Ray et al.[177] showing that Tfh effector cells exit the cell cycle earlier than Th1 cells.

Special attention was given to *Il7r* because it encodes the alpha chain of the IL-7R, which gives CD8^{+} MPECs a survival advantage during the contraction phase[27]. On day 6, the umap_1low *Mki67*$^{+}$ cycling cells lacked *Il7r*, some umap_1int cells expressed *Il7r*, and many but not all of the umap_1high cells expressed *Il7r* (Figure 4F). Surprisingly, *Il7r* expression was distributed across the X-axis (umap_1) of the umap_1int population rather than concentrated in day 6 cells that expressed the memory module. Moreover, very few day 6 cells expressing the Tfh module expressed *Il7r* including the cells that expressed the memory module. On days 21 and 60, nearly all cells expressing the Th1 module were *Il7r*$^{+}$ but many cells expressing the Tfh module had lower or no expression of *Il7r*. Overall, *Il7r* expression correlated less well with survival than expression of the memory

cell module. Therefore, in accordance with Marshall et al. 7, it is unlikely that expression of the IL-7R determined whether $CD4^+$ cells survived the contraction phase to become memory cells.

The transcriptional state of Th1 and Tfh cells is largely conserved from effector to memory phases.

The sequencing data was analyzed in more detail to further understand the relationship between the $CD4^+$ memory and effector T cells. We performed differential gene expression analysis in Seurat and identified 15 cell clusters with unique expression signatures across days 6, 21, and 60 (Figure 5A). Only a small number of *Foxp3*$^+$ Treg cells were detected as expected based on the flow cytometry results, and clustered with *Foxp3*$^–$ cells in cluster 8 (Figures 5A and 5B). Cells in cluster 12 had a type I interferon stimulated signature exemplified by expression of *Isg15* and did not change with time after aLm-2W infection. Treg cells and cluster 12 cells were not analyzed further. The cells in cluster 3, 4, 5, 6, 7, 9, 13, and 14 were predominantly umap_1lo and umap_1int effector cells, whereas cells

in clusters 0, 1, 2, 8, and 10, were predominantly umap_1hi memory cells (Figures 4E and 5A). Cells in cluster 11 were umap_1int effector cells on day 6 and umap_1hi memory cells on days 21 and 60.

Clusters 1, 5, 7, 8, 11, 13, and 14 contained cells that expressed the Th1 module (Figures 4E, 5A and 5B). Clusters 13 and 14 contained proliferating Th1 cells, whereas cluster 11 cells expressed *Cx3cr1* typical of terminally differentiated Th1 cells[178]. We confirmed by flow cytometry that cells expressing CX3CR1 indeed accounted for about 10% of the Ly-6C^{hi} Th1 population detected by flow cytometry (Figure 5C). Cells in effector cell cluster 5 and memory cell cluster 1 had similar umap_2 values and expressed *Ly6c2*, *Cxcr6*, *Selplg*, *Tbx21*, and *Ccl5* (Figure 5B) and thus corresponded to the Ly-6Chi Th1 effector and memory cells identified by flow cytometry. Likewise, cells in effector cell cluster 7 and memory cell cluster 8 had similar umap_2 values and expressed *Cxcr6*, *Selplg*, *Tbx21*, and *Ccl5* but less *Ly6c2* than cells in clusters 5 and 1 and were likely the Ly-6C^{lo} Th1 effector and memory cells. The main difference between the memory cells in clusters 1 and 8 was that cluster 8 expressed TRM genes such as *Itga1* 62 and *Rgs1* 63 while cells in cluster 1 expressed genes

involved in egress from lymphoid tissue (*Klf2*, *S1pr1*)[64]. These results align with the parabiosis results indicating that Ly-6C^{lo} Th1 memory cells are tissue resident while Ly-6C^{hi} Th1 memory cells recirculate (Figure 2D). Clusters 0, 2, 3, 4, 6, 9, and 10 contained cells that expressed the Tfh module (Figures 4E, 5A and 5B). Cells in effector cell cluster 4 and memory cell 10 expressed the Tfh genes *Cxcr5*,[53] and *Il6st* and the GC-Tfh genes *Tox2,*[77] and *Izumo1r* [184] and lacked *Klf2* and *S1pr1* involved in egress from lymphoid tissues[181] (Figure 5B). The cells in these clusters were therefore likely the SLO-resident GC-Tfh effector and memory cells identified by flow cytometry. Cells in clusters 3 and 6 were candidates for pre-Tfh or M-Tfh effector cells and cells in clusters 0 and 2 for the memory cell versions. Cells in all 4 clusters expressed *Selplg* but not *Ly6c2* or *Cxcr6* (Figure 5B) and had lower expression of *Cxcr5*, *Tox2,* and *Izumo1r* and higher expression of *Klf2* and *S1pr1* than the GC-Tfh cells in clusters 4 and 10. Although *Sell* was poorly detected in general, clusters 0, 2, 3, and 6 were the only clusters that contained cells that expressed *Ccr7*, which is under the same transcriptional control as *Sell*[181]. Therefore, clusters 3 and 6 likely contained a mixture of pre-Tfh and M-Tfh effector cells and clusters 0 and 2 a mixture of pre-Tfh and M-Tfh memory cells. This conclusion is bolstered

by the fact that the sum of the frequencies of pre-Tfh and M-Tfh memory cells among the tetramer+ population identified by flow cytometry was about the sum of the frequencies of cells in clusters 0 and 2 among the sequenced tetramer+ cells (Figure 5D). The fact that pre-Tfh and M-Tfh memory cells did not resolve into separate clusters is further evidence of the relatedness of these cell types. The few genes that differ between clusters 0, 2, 3, and 6, for example *Psmd3* and *Pgap1*, do not have obvious immunological functions and are under investigation. Cells in cluster 9 had similar amounts of *Cxcr5*, *Tox2*, and *Izumo1r* as cluster 3 and 6 cells but low amounts of *Klf2* and *S1pr1* like GC-Tfh cells. As described below, cluster 9 cells may have been pre-Tfh or M-Tfh effector cells in the process of becoming GC-Tfh cells.

Notably, the aLm-induced $CD4^+$ memory T cells did not preferentially express *Tcf7*, *Foxo1*, or *Myb* [185–188] as described for $CD8^+$ memory T cells. *Foxo1* was uniformly expressed in all $CD4^+$ effector and memory cell subsets, *Tcf7* was well expressed in all effector and memory cell subsets with highest expression in Tfh effector cells, and *Myb* was preferentially expressed in some of the Tfh subsets (Figure 5B). Rather, each $CD4^+$

effector and memory cell subset pair were segregated on the UMAP because the effector cells expressed the effector cell module typified by *Rilpl2* and *Gstt2* whereas the memory cells express the memory module typified by *Il7r*, *Vps37b*, and *Sspb2* (Figure 5B).

Secondary infection shows a Th1 progression towards CX_3CR1+ Th1.

The Th1 module showed a gradient of Th1 genes with the lowest expressing subset being the Ly6C^{lo} Th1, Ly6C^{hi} Th1 being intermediate and the CX3CR1^{+} Th1 subset with the highest Th1 genes. This raised the possibility that there is a progressive differentiation from Ly6C^{lo} Th1 to Ly6C^{hi} Th1 and finally to the terminally differentiated CX3CR1^{+} Th1 population. We tested this possibility by using the previously described adoptive transfer approach. 2W:I-A^{b} and LLOp:IA^{b} tetramer-enriched Ly-6C^{hi} Th1, Ly-6C^{lo} Th1, pre-Tfh, M-Tfh, and GC-Tfh memory cells were sorted from the SLOs of day 30 aLm-2W-infected mice (Figure 6A). The purity of the post-sort Ly-6C^{hi} Th1, Ly-6C^{lo} Th1, M-Tfh, and GC-Tfh populations was greater than 95 percent and the pre-Tfh population was greater than 90 percent (Figure 3B). The sorted cells were injected

intravenously into naïve mice expressing a different congenic marker, which were then infected with aLm-2W bacteria. The phenotypes of the transferred 2W:I-A^b tetramer-binding T cells were then determined 6 days later. Ly-$6C^{hi}$ Th1 memory cells mainly produced $CX3CR1^+$ Th1 and $Ly6C^{hi}$ Th1 secondary effector cells and very few cells of the Tfh variety. (Figures 6C and 6D). Ly-$6C^{lo}$ Th1 memory cells produced mostly Ly-$6C^{hi}$ Th1 secondary effector cells and some $CX3CR1^+$ and $Ly6C^{lo}$ Th1 cells, as well as some M-Tfh cells. The pre-Tfh memory cell donor population generated a secondary effector cell population of 30% M-Tfh, 20% GC-Tfh, and mostly $Ly6C^{lo}$ cells of the Th1 variety. M-Tfh memory cells mainly produced Ly-$6C^{lo}$ Th1 secondary effector cells and some M-Tfh and GC-Tfh cells, whereas GC-Tfh memory cells mainly produced GC-Tfh and $Ly6C^{lo}$ secondary effector cells. These results demonstrate that Th1 memory cells tend to differentiate from $Ly6C^{lo}$ to $Ly6C^{hi}$ and finally to $CX3CR1^+$ secondary effector cells and that both pre-Tfh and M-Tfh seem capable of generating $Ly6C^{lo}$ Th1 and M-Tfh and GC-Tfh populations while GC-Tfh largely remain GC-Tfh as secondary effector cells but they are not precluded from generating $Ly6C^{lo}$ Th1 effectors. Importantly, memory Pre-Tfh, M-Tfh and GC-Tfh were overall very poor at generating $CX3CR1^+$ Th1

cells. The Ly6C^{lo} Th1 cells preferred to become Ly6C^{hi} Th1 cells and the Ly6C^{hi} Th1 cells preferred to become CX3CR1^{+} Th1 secondary effectors providing evidence for a stepwise progression to Th1 cell differentiation.

Discussion

We created an unbiased list of genes that were upregulated at memory timepoints and selected genes that were expressed across all subsets. When the memory module list of genes was applied to the whole dataset there was a relatively small number of cells that were enriched for memory genes at day 6 and these cells had started to downregulate genes associated with effector cells. These cells are likely the MPEC cells that have been described for CD8^{+} T cells although they did not correlate with IL7R expression as demonstrated by Kaech et al[27]. There were also an even smaller number of cells at the effector time that occupied the same space as the memory cells. These cells appear to be the earliest memory cells and were mostly comprised of M-Tfh and Th1 cells. These cells express some of the effector module at D6 explaining why they do note

reside in memory umap space, but the number of cells that were present on the memory half of the plot makes it unlikely that these are the only cells that are capable of forming memory cells.

Overall, the transcriptome analysis supported the cell transfer results indicating that effector cell subsets generate phenotypically similar memory cell subsets. These results add to the plausibility that the cluster 5 Ly-6C^{hi} Th1 effector cells are the primary source of the transcriptionally related cluster 1 Ly-6C^{hi} Th1 memory cells, cluster 4 GC-Tfh effector cells are the primary source of cluster 10 GC-Tfh memory cells, cluster 7 Ly-6C^{lo} Th1 effector cells are the primary source of cluster 8 Ly-6C^{lo} Th1 memory cells, and cluster 3 and 6 pre-Tfh and M-Tfh effector cells are the primary source of cluster 0 and 2 pre-Tfh and M-Tfh memory cells.

Transferring memory cell subsets to naïve hosts that then received a secondary infection of aLm-2W showed that there is a progressive differentiation of Th1 subsets towards CX3CR1^{+} cells. While CX3CR1^{+} Th1 are relatively rare in a primary infection we found that Ly6C^{lo} Th1 produced Ly6C^{hi} Th1 and some CX3CR1^{+} Th1 cells, while Ly6C^{hi} Th1 cells largely produced CX3CR1^{+} secondary effector cells. This result is supported by the

Th1 module from the RNAseq where there is a gradient of the Th1 module with CX3CR1^{+} Th1 cells expressing the highest level of Th1 genes and Ly6C^{lo} Th1 cells expressing the lowest. Overall Pre-Tfh, M-Tfh and GC-Tfh were poor at generating CX3CR1^{+} Th1 cells but each of these populations generated some Ly6C^{lo} Th1 cells. In the RNAseq data set the most closely related Th1 subset to the Tfh subset is the Ly6C^{lo} Th1 cell suggesting that upon re-infection a Tfh like cell can become a Th1 but they do not complete the differentiation process and stall at the Ly6C^{lo} Th1 stage.

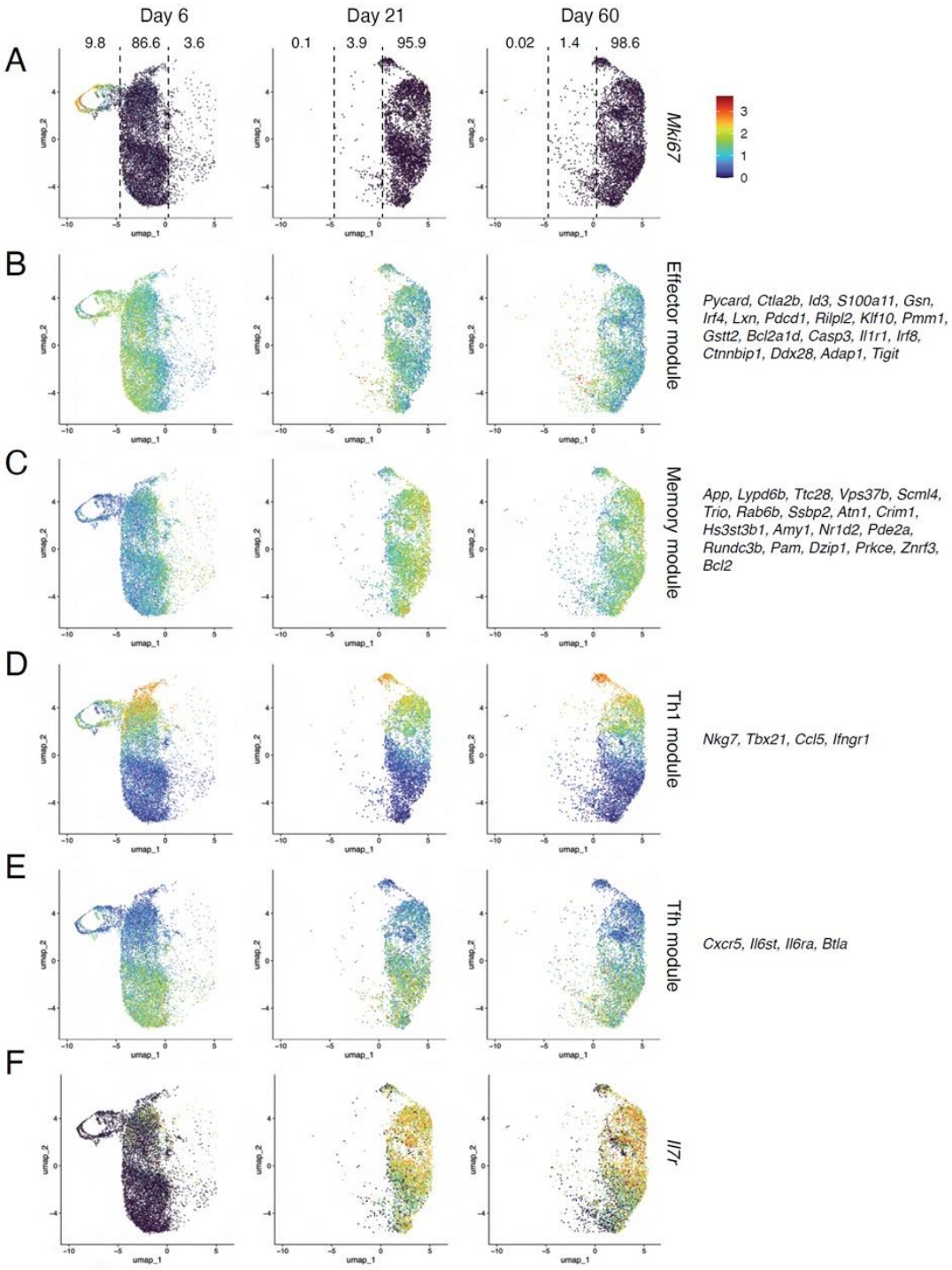
Day 6
Day 21
Day 60
A
9.8
86.6
3.6
0.1
3.9
95.9
0.02
1.4
98.6
Mki67
3
2
1
0
B
Effector module
Pycard, Ctla2b, Id3, S100a11, Gsn, Irf4, Lxn, Pdcd1, Rilpl2, Klf10, Pmm1, Gstt2, Bcl2a1d, Casp3, Il1r1, Irf8, Ctnnbip1, Ddx28, Adap1, Tigit
C
Memory module
App, Lypd6b, Ttc28, Vps37b, Scml4, Trio, Rab6b, Ssbp2, Atn1, Crim1, Hs3st3b1, Amy1, Nr1d2, Pde2a, Rundc3b, Pam, Dzip1, Prkce, Znrf3, Bcl2
D
Th1 module
Nkg7, Tbx21, Ccl5, Ifngr1
E
Tfh module
Cxcr5, Il6st, Il6ra, Btla
F
Il7r
umap_1
umap_2

Figure 4. Identification of CD4+ effector and memory T cells by single cell RNA sequencing.

(A) UMAP of single cell RNA sequencing data from 2W:I-A^b and LLOp:I-A^b tetramer+ cells FACS-sorted at the indicated times after aLm-2W infection featuring expression of *Mki67*. Percentages of cells in the umap_1low, umap_1int, or umap_1high intervals indicated by the dashed lines are shown above the plot. (B-F) UMAPs of single cell RNA sequencing data from 2W:I-A^b tetramer+ and LLOp:I-A^b tetramer+ cells FACS-sorted from the indicated times after aLm-2W infection featuring expression of an effector cell module of genes expressed to a greater extent on day 6 than day 21 (B), a memory cell module of genes expressed to a greater extent on day 21 than day 6 (C), a module of genes over-expressed in Th1 cells (D) or Tfh cells (E), or expression of *Il7r* (F).

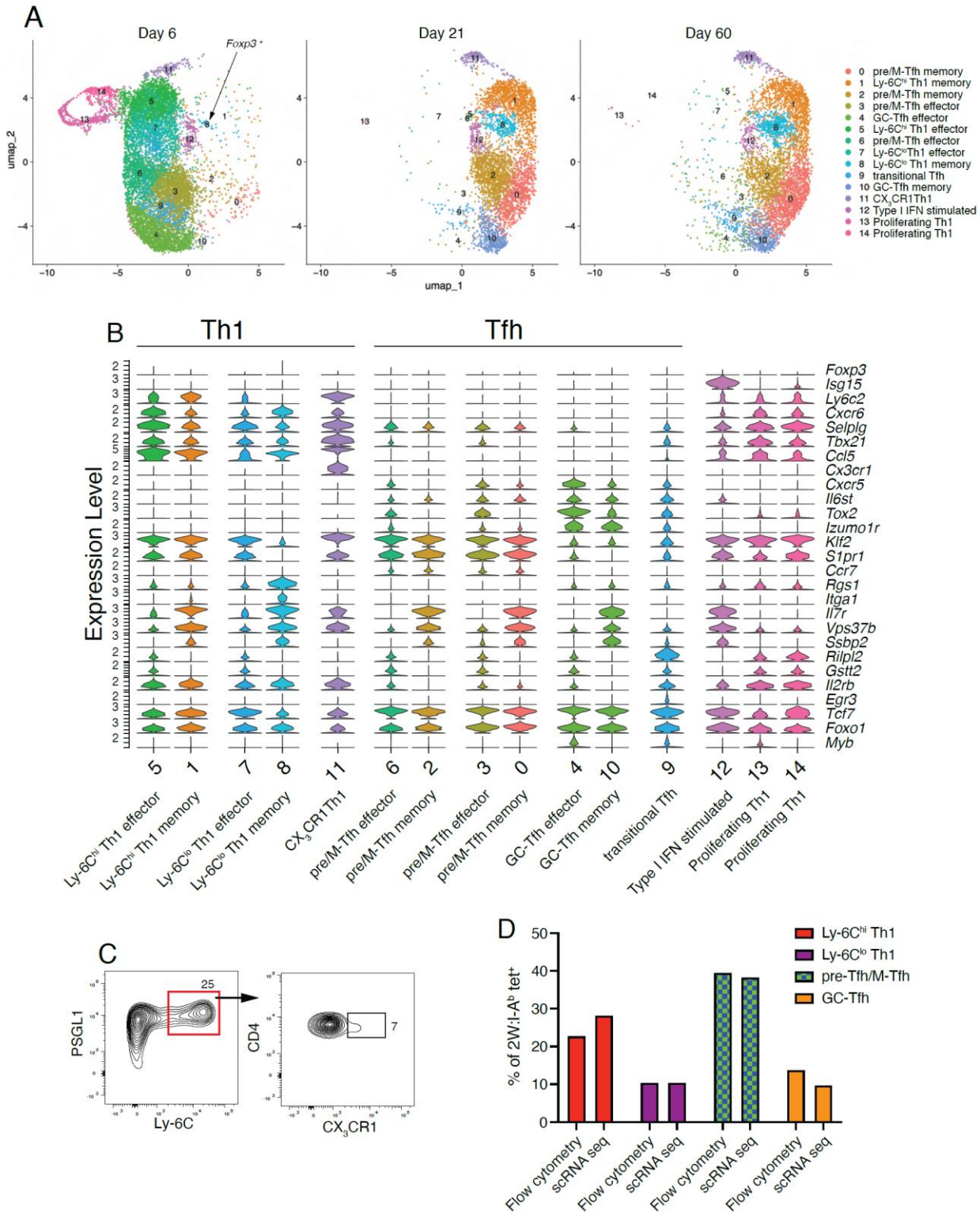
A
Day 6
Day 21
Day 60
Foxp3+
umap_1
umap_2
0 pre/M-Tfh memory
1 Ly-6C^hi Th1 memory
2 pre/M-Tfh memory
3 pre/M-Tfh effector
4 GC-Tfh effector
5 Ly-6C^hi Th1 effector
6 pre/M-Tfh effector
7 Ly-6C^hi Th1 effector
8 Ly-6C^lo Th1 memory
9 transitional Tfh
10 GC-Tfh memory
11 CX3CR1Th1
12 Type I IFN stimulated
13 Proliferating Th1
14 Proliferating Th1
B
Th1
Tfh
Expression Level
Foxp3
Isg15
Ly6c2
Cxcr6
Selplg
Tbx21
Ccl5
Cx3cr1
Cxcr5
Il6st
Tox2
Izumo1r
Klf2
S1pr1
Ccr7
Rgs1
Itga1
Il7r
Vps37b
Ssbp2
Rilpl2
Gstt2
Il2rb
Egr3
Tcf7
Foxo1
Myb
5 1 7 8 11 6 2 3 0 4 10 9 12 13 14
Ly-6C^hi Th1 effector
Ly-6C^hi Th1 memory
Ly-6C^lo Th1 effector
Ly-6C^lo Th1 memory
CX3CR1Th1
pre/M-Tfh effector
pre/M-Tfh memory
pre/M-Tfh effector
pre/M-Tfh memory
GC-Tfh effector
GC-Tfh memory
transitional Tfh
Type I IFN stimulated
Proliferating Th1
Proliferating Th1
C
PSGL1
Ly-6C
25
CD4
CX3CR1
7
D
% of 2W:I-A^b tet+
Ly-6C^hi Th1
Ly-6C^lo Th1
pre-Tfh/M-Tfh
GC-Tfh
Flow cytometry
scRNA seq

Figure 5. Identification of Th1 and Tfh effector and memory cell subsets by single cell RNA sequencing.

(A) Dimension reduction plot of single cell RNA sequencing data from 2W:I-A^b and LLOp:I-A^b tetramer+ cells FACS-sorted from the indicated times after aLm-2W infection with identity calls on each cluster listed in the legend. (B) Violin plots of expression of the indicated genes by the indicated Th cell subsets. (C) Flow cytometry plots of the indicated molecules on 2W:I-A^b tetramer+ cells from aLm-2W-infected mice demonstrating the presence of CX3CR1$^+$ cells in the Ly-6C^{hi} Th1 cell subset. (D) 2W:I-A^b plus LLOp:I-A^b tetramer-binding T cells sorted from the spleens of day 21 and 60 aLm-2W infected mice were analyzed by single cell RNA sequencing or by flow cytometry and memory cells subsets were identified as described in Figure 5A and Figure 2A. The values in the table indicate the percentage of each subset in the tetramer-binding population identified by each method.

Genes	p_val	avg_log2FC	pct.1	pct.2	p_val_adj	PcDiff
Hist1h1b	1.82E-240	4.079857211	0.142	0.015	3.95E-236	0.127
Stmn1	1.49E-279	3.631925569	0.213	0.045	3.23E-275	0.168
Mki67	1.10E-263	3.6058583	0.174	0.026	2.39E-259	0.148
Hist1h2ae	2.21E-240	3.506221526	0.195	0.043	4.79E-236	0.152
S100a4	0	2.827916468	0.744	0.273	0	0.471
Top2a	0	2.812710547	0.252	0.055	0	0.197
Cks1b	1.91E-116	2.621278734	0.102	0.023	4.15E-112	0.079
Gzmb	1.32E-174	2.615734507	0.129	0.023	2.87E-170	0.106
E2f2	0	2.599183938	0.258	0.045	0	0.213
Hist1h2ap	1.38E-265	2.577469484	0.414	0.183	3.00E-261	0.231
Gsn	4.34E-200	2.439257975	0.14	0.022	9.43E-196	0.118
Lgals3	3.11E-146	2.265509321	0.129	0.03	6.76E-142	0.099
Tox2	0	2.243098592	0.465	0.126	0	0.339
Anxa2	0	2.223398198	0.446	0.133	0	0.313
Slc36a3os	1.72E-181	2.222194414	0.142	0.028	3.73E-177	0.114
Id3	0	2.196662814	0.315	0.088	0	0.227
Irf4	9.54E-211	2.171669985	0.191	0.048	2.07E-206	0.143
Gzmk	2.69E-226	2.128917002	0.202	0.051	5.84E-222	0.151
Il1r1	1.16E-123	2.119306235	0.102	0.021	2.53E-119	0.081
Ctla2b	7.65E-151	1.982291852	0.145	0.038	1.66E-146	0.107
Irf8	2.06E-90	1.952673705	0.101	0.03	4.46E-86	0.071
Ptms	0	1.903894992	0.289	0.076	0	0.213
S100a6	0	1.833800029	0.933	0.668	0	0.265
Ptrh1	1.44E-125	1.819520517	0.128	0.035	3.13E-121	0.093
Klc3	1.91E-110	1.808662124	0.101	0.024	4.16E-106	0.077
Rapgef5	1.38E-160	1.788555226	0.169	0.049	2.98E-156	0.12
Cks2	4.39E-224	1.747209971	0.254	0.084	9.52E-220	0.17
Ctla2a	1.02E-269	1.736991252	0.515	0.31	2.22E-265	0.205
Cenpa	1.68E-231	1.735318293	0.317	0.127	3.64E-227	0.19
Dtl	9.52E-112	1.689118454	0.131	0.041	2.07E-107	0.09
Lxn	4.37E-135	1.687271683	0.137	0.037	9.49E-131	0.1
Cenpw	4.11E-110	1.668747534	0.123	0.037	8.93E-106	0.086
Pdcd1	3.36E-168	1.667985231	0.185	0.056	7.29E-164	0.129
Racgap1	2.57E-135	1.662942011	0.159	0.051	5.59E-131	0.108

Table 2. Effector gene list

List of genes that were expressed at least 2-fold greater in day 6 (pct.1) than day 21 (pct.2) 2W:I-Ab and LLOp:I-A^b tetramer-binding cells from aLm-2W infected mice and in at least 10% of the effector. The genes used to produce the effector cell module are highlighted in yellow. These genes were chosen because of uniform expression across the day 6 Th subsets.

Genes	p_val	avg_log2FC	pct.1	pct.2	p_val_adj	PcDiff
Samd3	4.19E-162	-3.09704969	0.017	0.103	9.10E-158	-0.086
Coro2a	2.04E-166	-3.07841686	0.032	0.133	4.43E-162	-0.101
Il7r	0	-3.05653311	0.251	0.85	0	-0.599
App	3.96E-139	-2.50636469	0.026	0.112	8.59E-135	-0.086
Lypd6b	1.01E-191	-2.37035803	0.039	0.158	2.19E-187	-0.119
Dse	3.68E-112	-2.27176477	0.03	0.106	7.98E-108	-0.076
Ttc28	8.63E-263	-2.11067271	0.076	0.244	1.87E-258	-0.168
Myo3b	5.74E-129	-2.06837326	0.055	0.152	1.25E-124	-0.097
Fasl	1.79E-174	-2.00142926	0.054	0.174	3.89E-170	-0.12
Vps37b	0	-1.97025864	0.411	0.753	0	-0.342
Tdrp	1.71E-105	-1.93230625	0.034	0.109	3.72E-101	-0.075
Scml4	0	-1.91921969	0.271	0.628	0	-0.357
Trio	7.85E-135	-1.8900995	0.063	0.167	1.70E-130	-0.104
Rab6b	5.30E-168	-1.85985799	0.066	0.188	1.15E-163	-0.122
Ddx60	7.30E-195	-1.85548	0.107	0.255	1.58E-190	-0.148
Ssbp2	0	-1.84099115	0.21	0.51	0	-0.3
Atn1	1.13E-91	-1.81111754	0.042	0.114	2.46E-87	-0.072
Abcb1a	0	-1.78931525	0.262	0.507	0	-0.245
Crim1	0	-1.74540524	0.214	0.475	0	-0.261
Atp8b4	4.38E-182	-1.73369314	0.15	0.302	9.51E-178	-0.152
Acoxl	8.47E-72	-1.72178115	0.044	0.107	1.84E-67	-0.063
Chrm3	5.21E-76	-1.69399979	0.046	0.113	1.13E-71	-0.067
Itga1	8.25E-62	-1.68747205	0.063	0.127	1.79E-57	-0.064
Crim1	2.37E-98	-1.64317862	0.052	0.134	5.15E-94	-0.082
Tent5a	1.21E-119	-1.60814239	0.067	0.167	2.63E-115	-0.1
A330040F15Rik	8.34E-62	-1.59922197	0.061	0.124	1.81E-57	-0.063
Hs3st3b1	7.63E-172	-1.59123522	0.112	0.252	1.66E-167	-0.14
Acvr2a	5.50E-52	-1.57936293	0.049	0.101	1.19E-47	-0.052
Amy1	4.78E-67	-1.56922254	0.05	0.112	1.04E-62	-0.062
Dstyk	2.22E-72	-1.52694002	0.05	0.117	4.82E-68	-0.067
Ifit1bl1	6.19E-86	-1.50443123	0.069	0.15	1.34E-81	-0.081
Nr1d2	2.16E-137	-1.49855902	0.093	0.21	4.69E-133	-0.117
Usp18	4.41E-44	-1.49510697	0.065	0.117	9.56E-40	-0.052
Gm35188	7.93E-108	-1.47686833	0.081	0.179	1.72E-103	-0.098

Table 3. Memory gene list

List of genes that were expressed at least 2-fold greater in day 21 (pct.2) than day 6 (pct.1) 2W:I-A^b and LLOp:I-A^b tetramer-binding cells from aLm-2W infected mice and in at least 10 % of the memory cells. The avg_log2FC values are negative because the comparison was done by dividing the day 6 values by the day 21 values. The genes used to produce the memory cell module are highlighted in yellow. These genes were chosen because of uniform expression across the day 21 Th subsets.

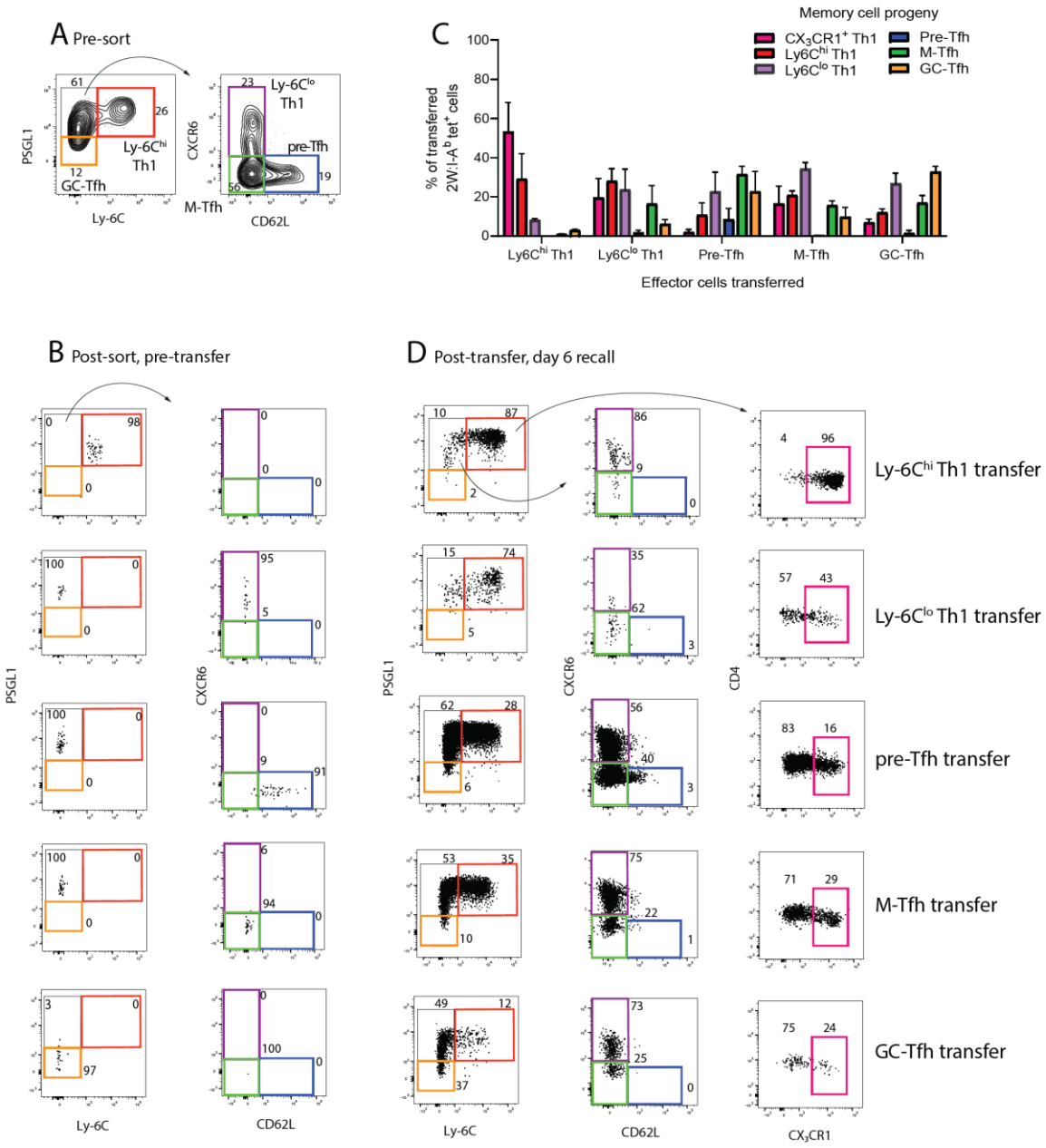

Figure 6. Secondary infection shows a progression of Th1 differentiation.

(A) Representative flow cytometry plots of the indicated molecules on 2W:I-A^b tetramer+ cells from the SLOs of CD45.2+ mice, 30 days after aLm-2W infection from a sample later subjected to FACS sorting. (B) Flow cytometry plots of the indicated molecules on 2W:I-A^b tetramer+ effector cells of the indicated subsets from SLOs of day 30 aLm-2W-infected CD45.2+ mice after FACS sorting based on the gates shown in (A). (C) Mean percentages (±} SEM, n ≥ 3 from 4 independent experiments) of 2W:I-A^b tetramer-binding secondary effector cell subsets of CD45.2+ donor origin in CD45.1+ mice that received the indicated FACS-sorted CD45.2+ effector cell populations 6 days earlier. (D) Flow cytometry plots of the indicated molecules on 2W:I-A^b tetramer+ secondary effector cells derived from the indicated FACS-sorted memory cell subsets 6 days after transfer and reinfection in naive recipients.

Chapter 5. CD4+ memory T cell subsets vary in their dependence on IL-7, IL-15 and TCR signaling for survival.

The increase in *Il7r* expression in the memory cell populations was consistent with the well-established fact that IL-7R plays a role in memory cell survival[128]. Given, however, that the earlier work was done on bulk $CD4^+$ memory T cells it seemed important to confirm this concept for all memory subsets. The role of IL-7R was assessed using *Cd4 Cre-ERT2 Il7r fl/fl* mice in which administration of tamoxifen results in deletion of the *Il7r* gene encoding the IL-7R alpha chain. *Cd4 WT/Cre-ERT2 Il7r fl/fl* mice or *Cd4 WT/WT Il7r fl/fl* controls were infected with aLm-2W bacteria and then treated on day 50 with tamoxifen for 1 week. One month later, the Ly-$6C^{hi}$ Th1, Ly-$6C^{lo}$ Th1, M-Tfh, and pre-Tfh memory cell populations cells were significantly smaller in *Cd4 WT/Cre-ERT2 Il7 fl/fl* mice than in the *Cd4 WT/WT Il7r fl/fl* controls (Figure 6A) and the GC-Tfh memory cells were diminished but not to the point of statistical significance. The minimal effect of IL-7R loss on GC-Tfh memory cells may have been related to these cells expressing less *Il7r* than other memory cells (Figure 5B).

The relatively minor effect of IL-7R ablation on GC-Tfh memory cells warranted assessment of IL-15, another cytokine implicated in the survival of $CD4^+$ memory T cells.12 Mice lacking IL-15, which is sensed by a receptor consisting of the IL-15 receptor alpha chain, IL-2/IL-15 receptor beta chain, and the common gamma chain[189] were used for this purpose. Ly-$6C^{lo}$ Th1 memory cells were the only subset to be substantially reduced in aLm-2W-infected IL-15-deficient mice compared to controls (Figure 6B) even though Ly-$6C^{hi}$ Th1 memory expressed as much *Il2rb*, which encodes the IL-2/IL-15 receptor beta chain (Figure 5B). A clue about the maintenance of GC-Tfh memory cells was present in the single cell RNA sequencing data. Although very few umap_1int cells were present on days 21 and 60, the few that were present were transitional Tfh cells in cluster 9, which expressed the TCR-induced gene, *Egr3* [31], and lacked *Il7r* [130] indicative of ongoing TCR signaling (Figure 5B). It was therefore possible that a source of aLm-derived peptide:MHCII complexes, perhaps GC B cells [47], was present even on day 60 and driving a loop in which Tfh cells were cycling between transitional Tfh (cluster 9), GCTfh effector (cluster 4), and GC-Tfh memory cells (cluster 10). Attempts to address this possibility by blocking I-A^b MHCII molecules with the Y3P monoclonal antibody were

foiled by the fact that this treatment depleted most I-A^{b+} cells (KCO, unpublished observation). Instead, we utilized the YTS177 CD4 monoclonal antibody, which is known to block CD4-dependent T cell activation without depleting all $CD4^+$ T cells.[191] Mice were infected with aLm-2W bacteria and on day 30 treated with YTS177 or isotype-control antibody for 2 weeks. YTS177 antibody treatment reduced the frequency of GC-Tfh but no other memory cell subset in the 2W:I-A^b or LLOp:I-A^b tetramer-binding population (Figure 6C). Therefore, CD4-assisted TCR activation was required for maintenance of GC-Tfh memory cells or their phenotype. One explanation for this phenomena was that GC-Tfh cells were maintained by TCR signals from antigen-presenting cells in GCs were GC-Tfh cells normally reside[53]. As expected, about 30 percent of the follicles in the spleens of mice infected intravenously with aLm-2W 14 days earlier contained GCs, whereas GCs were rare in the spleens of uninfected mice (Figures 6D and 6E). Remarkably, however, about 20 percent of the splenic follicles still contained GCs 60 days after aLm-2W infection. Thus, it is possible that the GC-Tfh memory cells were maintained by TCR stimulation in response to aLm-2W-derived peptide:MHCII complexes in GCs.

Discussion

Survival of memory $CD4^+$ T cells has largely been described to rely on IL7 or IL15 signaling, but the reliance of newly appreciated subsets on these cytokines has not been investigated. By applying our phenotyping panel to inducible IL7r knockout mice we confirmed that most subsets are reliant upon IL7r signaling to maintain their cellular numbers. GC-Tfh were the exception showing no decline over the course of the experiment. We tested if this resident subset was using IL15 to survive but only the resident $Ly6C^{lo}$ Th1 showed a small but significant decline in the absence of IL15. We hypothesized that the GC-Tfh population may be sensitive to latent antigen that could be maintained in germinal centers.

To test this hypothesis, we blocked CD4 with a non-depleting antibody and found that after 2 weeks of CD4 inhibition there was a significant decrease in the number of GC-Tfh cells. This suggested that there were lingering germinal centers after aLM-2W infection that could maintain this subset through CD4 assisted TCR signaling. By imaging sections and staining for GL7 on B cells we found an increased number of germinal centers at both

day 14 and day 60 when compared to uninfected controls. This evidence supports the idea that long lasting germinal centers are providing latent antigen to memory GC-Tfh maintaining their survival over time.

Overall, most memory $CD4^+$ T cells relied on IL7r signaling to survive with the $Ly6C^{lo}$ Th1 also being minorly dependent on IL15 and the GC-Tfh using a surprising strategy of antigen sensing to maintain their survival. The cells providing antigen remain elusive but the persistence of GC structures after an acute bacterial infection provides evidence that perhaps limited antigen presentation within the latent GC structures sustains long lived GC-Tfh survival. Kunzli et al.[47] suggest that preventing long lived GC-Tfh interaction with memory B cells through ICOSL blocking experiments decreases the overall titers of IgG within the host but whether or not these processes have any protective roles in the host remain to be studied.

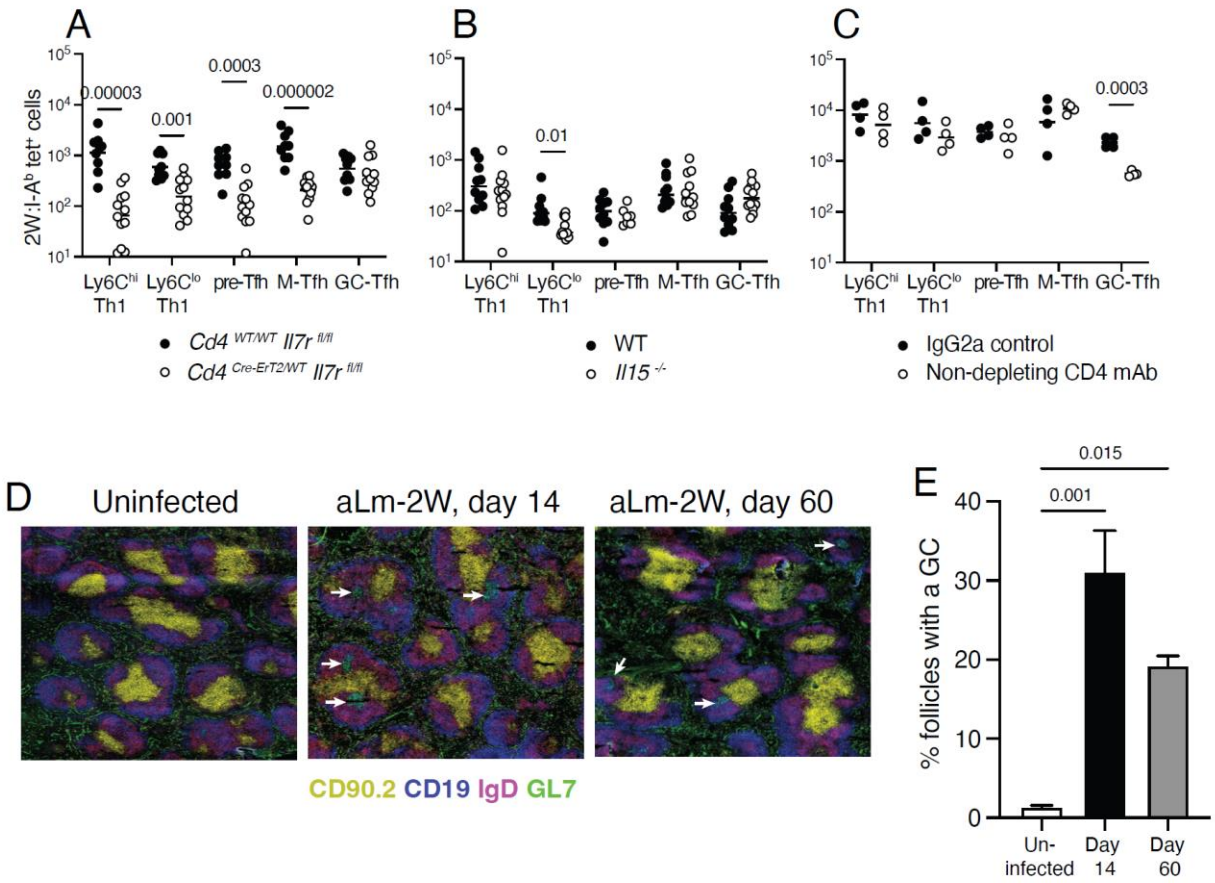

Figure 6. Memory T cell subsets depend on IL-7 and/or IL-15 or CD4 for survival.

(A) Numbers of 2W:I-A^b tetramer-binding cells of the indicated memory subsets from the SLOs of individual *Cd4 WT/WT Il7r fl/fl* (filled circles) or *Cd4 Cre-ERT2/WT Il7r fl/fl* (open circles) mice (n ≥ 5 from 4 independent experiments) 50 days after aLm-2W infection, and 30 days after tamoxifen treatment. Mean values are indicated with a horizontal bar. P values from a

Multiple T test. (B) Numbers of 2W:I-A^b tetramer-binding cells of the indicated memory subsets from the SLOs of individual wild-type (filled circles) or *Il15 -/-* (open circles) mice (n ≥ 8 from 4 independent experiments) 30 days after aLm-2W infection. Mean values are indicated with a horizontal bar. P values from a Multiple T test. (C) Numbers of 2W:I-A^b tetramer-binding cells of the indicated memory subsets from mice infected with aLm-2W bacteria and then 40 days later, injected twice intraperitoneally with YTS177 CD4 antibody or control IgG, seven days apart and analyzed seven days after the second antibody injection. Mean values are indicated with a horizontal bar. P values from a Multiple T test. (D) Fluorescence microscope images of spleen from uninfected mice or mice infected intravenously with aLm-2W bacteria for 14 or 60 days before analysis. Staining with CD90.2 (yellow) identified T cell areas. Follicles were identified as dense collections of IgD+ (purple) CD19+ (blue) cells and GCs as foci of CD19+ GL7+ cells (bluish green) within follicles. (E) Mean percentages (±} SD, n = 2 sections averaged from 3 mice per group) of follicles containing a GC in the spleens of mice from the indicated groups. P values were derived from a one-way ANOVA with a Tukey's multiple comparisons test.

Chapter 6: Concluding remarks

The goal of this research was to better understand how $CD4^+$ memory T cells are generated. Our results show that aLm-2W-induced naive $CD4^+$ T cells rapidly generate a large population of Th1 and Tfh effector cells, which peaks 6 days after infection. At this time, about 90 percent of the cells in both subsets expressed transcriptomes enriched for genes involved in cell stress and death. About 4 percent of the cells, however, expressed a transcriptome enriched for genes involved in cell quiescence and survival and shared by later memory cells and another 10 percent were trending in this direction. These results are consistent with the possibility that the cells with stress and death prone transcriptomes on day 6 died during the contraction phase, while the cells with quiescence and survival prone transcriptomes lived to become memory cells. This model raises the question of what factor causes a minority of effector cells to become memory cells. Research on $CD8^+$ T cells indicates that memory cells are derived from MPECs marked by early expression of the IL-7R. Marshall et al.[39], however, showed that IL-$7R^-$ and IL-$7R^+$ $CD4^+$ effector cells generated memory cells with the same efficiency. Likewise, we found that

about the same fraction of day 6 Th1 and Tfh effector cells became memory cells equally despite a greater fraction of the Th1 population expressing the IL-7R at the time when the contraction began. Rather than early expression of the IL-7R, the key to $CD4^+$ memory cell survival appears to be rapid acquisition of a quiescence program. The effector cells that become quiescent earlier than others may be exposed to less activation-associated macromolecular damage and therefore gain a survival advantage. Some effector cells may exit the cell cycle before others because of early disengagement from antigen-presenting cells or because of an intrinsic property of their TCRs, for example, weak activation due to low affinity the agonist peptide:MHCII ligand or tuning due to a TCR with a higher-than-average affinity for a self peptide:MHCII ligand. Conversely, cells with high affinity TCRs may experience intense TCR signaling that causes premature induction of an inhibitory pathway. The facts that an inverse relationship between memory cell formation and proliferation has been observed in other studies[192,193], and rapamycin, an Mtor and proliferation blocking drug[194], enhances memory cell formation favor this model. The results indicate that $CD4^+$ effector cells retain their Th1 of Tfh identities once becoming memory cells. The most compelling

evidence supporting this contention is that purified effector cell subsets generated memory cells with the same cell surface phenotype after transfer into infection matched recipients. This relationship was not perfect, however. Although Ly-6C^{hi} Th1 effector cells generated memory cells with that phenotype, they also generated some Ly-6C^{lo} Th1 and M-Tfh memory cells. Along this line, Hu et al.[195] showed that Ly-6C^{hi} Th1 memory cells can generate Ly-6C^{lo} Th1 effector cells during the secondary response. The capacity of T-bet-dependent Ly-6C^{hi} Th1 effector cells to produce Ly-6C^{lo} Th1 and M-Tfh memory cells may explain the small reductions in these populations in T-bet-deficient mice. The fact, however, that T-bet deficiency had only a small effect on the Ly-6C^{lo} Th1 population suggests that T-bet independent Ly-6C^{lo} Th1 effector cells are the main source of Ly-6C^{lo} Th1 memory cells. Other work has shown that Ly-6C^{hi} Th1 cells can also generate terminally differentiated CX3CR1^{+} Th1 cells[178], which made up a small fraction of aLm-2W-induced effector cells population. We therefore tested the possiblity that Ly-6C^{lo} Th1 effector cells are capable of forming Ly6C^{hi} Th1 cells that then produce CX3CR1^{+} Th1 cells in a secondary infection. The secondary infection experiments suggest that the progressive differentiation of Th1 subsets from Ly6C^{lo} to Ly6C^{hi} and finally

to CX3CR1^{+} Th1 cells is a somewhat stepwise progression. Tfh cells were relatively poor at forming CX3CR1^{+} Th1 cells, but formed some Ly6C^{lo} Th1 cells further suggesting that Tfh memory cells are not poised to complete the Th1 differentation process. Evidence for progressive differentiation was also found for Tfh cells. CXCR5^{+} pre-Tfh cells, which were defined by expression of the naive T cell marker CD62L, may be recently activated naive cells. Additional TCR signaling may induce Bcl-6 in these cells causing differentiation into M-Tfh cells. More prolonged TCR signaling, perhaps triggered by interactions with GC B cells, may cause the M-Tfh cells to generate GC-Tfh effector cells. The fact that all the effector cell types were present at the same time on day 6 could be related to a sudden reduction in antigen presentation as the bacteria are cleared around this time. The associated cessation of TCR signaling may prevent the less differentiated cells in the progression from differentiating further and trigger transition to the memory cell state. This research also shed light on the functions and migration behaviors of the Th1 cells induced by acute systemic bacterial infection. The Ly-6C^{hi} Th1 cells, originally identified by Marshall et al.[39], depended on T-bet to form, produced mRNA encoding IFN-γ, circulated through SLOs, and migrated to the liver. These cells

therefore fit the classical definition of TEM cells[126] and likely function as recruitable macrophage activators. We also identified the enigmatic Ly-6C^{lo} cells that expressed T-bet but formed in a relatively T-bet-independent manner and resemble cells described in several studies on the immune response to *Toxoplasma gondii*[196,197]. These cells were transcriptionally similar to the Ly-6C^{hi} Th1 cells but differed by lacking *Klf2* and *S1pr1* needed for egress from tissues[181] and expressing *Itga1*[179] (encoding the alpha chain of CD49a) and *Rgs1*[7], which are associated with tissue residence. These facts, together with the observations that Ly-6C^{lo} Th1 cells were progressively lost from the blood and migrated slowly into joined parabionts suggest that Ly-6C^{lo} Th1 cells are TRM cells in the SLOs and probably the liver. Although CD4^{+} effector T cells may not require IL-7R expression to become memory cells, our data show that most CD4^{+} memory T cells re-express it, and Ly-6C^{hi} Th1, Ly-6C^{lo} Th1, pre-Tfh, and M-Tfh memory cells use it to survive. Ly-6C^{lo} Th1 TRM cells also required IL-15 for optimal survival, perhaps because of a need for more STAT5 signals, which are transduced by both IL-7R and IL-15R [198], than other memory cell types. IL-15 is also required for the survival of some types of CD8^{+} TRM cells[199] suggesting that TRM may live in IL-15-rich niches. GC-Tfh memory

cells differed from the other memory cell types by being less dependent on IL-7 and by requiring CD4-assisted TCR signaling to survive or maintain their phenotype. It is possible that this TCR signaling is driven by self peptide:MHCII ligands or of the tonic variety described for B cells[200,201]. Another possibility, based on Kunzli et al.[47] and our finding that GCs are still present 2 months after infection, is that GC B cells specific for the aLm antigens, acquire this material from follicular dendritic cells, which can store injected proteins bound to antibodies or comlement fragments for months[202–204]. These GC B cells may then stimulate the TCRs on aLm peptide:MHCII-specific GC-Tfh memory cells causing them to become transitional Tfh cells (cluster 9), which eventually disengage from the B cells and return to the GC-Tfh memory cell state (cluster 10). Interestingly, transitional Tfh cells did not express *Mki67* on day 60 despite strong expression of the effector cell module indicating that conversion between the transitional Tfh and GC-Tfh memory cell states does not involve proliferation, perhaps because of expression of inhibitory receptors such as PD-1. In any case, the long-term maintenance of GC-Tfh cells by a TCR-dependent process indicates that these cells are not remembering the antigen, but rather are being reminded by it.

The aLm peptide:MHCII-specific T cells that expressed the effector module and accounted for 90 percent of the effector cell population on day 6 may have all died during the contraction phase, and thus behaved like SLECs, while the minority population that expressed the memory module, may have survived, and thus behaved like MPECs. The fact that the $CD4^+$ memory T cells that were present at day 6, 21, or 60 had basically the identical transcriptomes suggests that these cells do not undergo the progressive differentiation described for $CD8^+$ T cells.[205] In addition, the $CD4^+$ memory T population described here did not contain a small subset of *Tcf7*$^+$ stem-like cells, which maintain the $CD8^+$ TCM subset[206] Rather, $CD4^+$ T cells rapidly become Th1 or Tfh effector cells, most of which express a death promoting transcriptome. A minority of cells of both types, however, quickly lose the death program and turn on a survival program to avoid cell death. These cells then survive as stable memory cells by sensing IL-7 or by intermittent TCR signaling in response to peptide:MHCII ligands, perhaps contained only in GCs.

REFERENCES

1. Riedel S. (2005). Edward Jenner and the history of smallpox and vaccination. Proc. Bayl. Univ. Med. Cent 18, 21–25. [PubMed: 16200144]

2. Ahmed R, and Gray D. (1996). Immunological memory and protective immunity: understanding their relation. Science 272, 54–60. 10.1126/science.272.5258.54. [PubMed: 8600537]

3. Rudolph MG, Stanfield RL, and Wilson IA (2006). How TCRs bind MHCs, peptides, and coreceptors. Annu. Rev. Immunol 24, 419–466. [PubMed: 16551255]

4. Jenkins MK, Khoruts A, Ingulli E, Mueller DL, McSorley SJ, Reinhardt RL, Itano A, and Pape KA (2001). In vivo activation of antigen-specific CD4 T cells. Annu. Rev. Immunol 19, 23–45. [PubMed: 11244029]

5. Zhu J, and Paul WE (2010). Heterogeneity and plasticity of T helper cells. Cell Res. 20, 4–12. cr2009138 [pii] 10.1038/cr.2009.138. [PubMed: 20010916]

6. Ruterbusch M., Pruner KB., Shehata L., and Pepper M. (2020). In vivo CD4+ T cell dDifferentiation and function: revisiting the Th1/Th2 paradigm. Annu. Rev. Immunol 38, 705–725. 10.1146/annurev-immunol-103019-085803. [PubMed: 32340571]

7. Crotty S. (2011). Follicular helper CD4 T cells (TFH). Annu. Rev. Immunol 29, 621–663. 10.1146/annurev-immunol-031210-101400. [PubMed: 21314428]

8. Freeborn RA, Strubbe S, and Roncarolo MG (2022). Type 1 regulatory T cell-mediated tolerance in health and disease. Front. Immunol 13, 1032575. 10.3389/fimmu.2022.1032575.

9. Tuzlak S, Dejean AS, Iannacone M, Quintana FJ, Waisman A, Ginhoux F, Korn T, and Becher B. (2021). Repositioning TH cell polarization from single cytokines to complex help. Nat. Immunol 22, 1210–1217. 10.1038/s41590-021-01009-w. [PubMed: 34545250]

10. Yoshitomi H. (2022). Peripheral helper T cell responses in human diseases. Front. Immunol 13, 946786. 10.3389/fimmu.2022.946786.

11. Pepper M, and Jenkins MK (2011). Origins of CD4(+) effector and central memory T cells. Nat. Immunol 131, 467–471. ni.2038 [pii] 10.1038/ni.2038.

12. Jameson SC, and Masopust D. (2018). Understanding subset diversity in T cell memory. Immunity 48, 214–226. 10.1016/j.immuni.2018.02.010. [PubMed: 29466754]

13. Sallusto F, Lenig D, Forster R, Lipp M, and Lanzavecchia A. (1999). Two subsets of memory T lyMPEChocytes with distinct homing potentials and effector functions. Nature 401, 708–712. [PubMed: 10537110]

14. Ciabattini A, Pettini E, and Medaglini D. (2013). CD4+ T cell priming as biomarker to study immune rResponse to preventive vaccines. Front. Immunol 4, 421. doi: 10.3389/fimmu.2013.00421. [PubMed: 24363656]

15. Dileepan T, Malhotra D, Kotov DI, Krueger PD, Kolawole EM, Evavold BD, and Jenkins MK (2021). MHC class II tetramers engineered for enhanced CD4 binding outperform conventional tetramers for detection of antigen-specific T cells. Nat Biotechnol. 8, 943–948. 10.1038/s41587-021-00893-9.

16. Landais E, Romagnoli PA, Corper AL, Shires J, Altman JD, Wilson IA, Garcia KC, and Teyton L. (2009). New design of MHC class II tetramers to accommodate fundamental principles of antigen presentation. J Immunol 183, 7949–7957. [PubMed: 19923463]

17. Doherty PC (2011). The tetramer transformation. J. Immunol 187, 5–6. 10.4049/jimmunol.1101297. [PubMed: 21690330]

18. Hataye J, Moon JJ, Khoruts A, Reilly C, and Jenkins MK (2006). Naive and memory CD4+ T cell survival controlled by clonal abundance. Science 312, 114–116. [PubMed: 16513943]

19. Marzo AL., Klonowski KD., Le Bon A., Borrow P., Tough DF., and Lefrancois L. (2005). Initial T cell frequency dictates memory CD8+ T cell lineage commitment. Nat. Immunol 6, 793–799. [PubMed: 16025119]

20. Lee H-G, Cho M-Z, and Choi J-M (2020). Bystander CD4+ T cells: crossroads between innate and adaptive immunity. Exp. Mol. Med 52, 1255–1263. 10.1038/s12276-020-00486-7. [PubMed: 32859954]

21. Moon JJ, Chu HH, Pepper M, McSorley SJ, Jameson SC, Kedl RM, and Jenkins MK (2007). Naive CD4(+) T cell frequency varies for different epitopes and predicts repertoire diversity and response magnitude. Immunity 27, 203–213. [PubMed: 17707129]

22. Pepper M, Pagán AJ, Igyártó BZ, Taylor JJ, and Jenkins MK (2011). Opposing signals from the Bcl6 transcription factor and the interleukin-2 receptor generate T helper 1 central and effector memory cells. Immunity 35, 583–595. 10.1016/j.immuni.2011.09.009. [PubMed: 22018468]

23. Pepper M, Linehan JL, Pagán AJ, Zell T, Dileepan T, Cleary PP, and Jenkins MK (2010). Different routes of bacterial infection induce long-lived TH1 memory cells and short-lived TH17 cells. Nat. Immunol 11, 83–89. 10.1038/ni.1826. [PubMed: 19935657]

24. Sabatino J, Huang J, Zhu C, and Evavold BD (2011). High prevalence of low affinity peptide–MHC II tetramer–negative effectors during polyclonal CD4+ T cell responses. J. Exp. Med 10.1084/jem.20101574.

25. Murali-Krishna K, Altman JD, Suresh M, Sourdive DJ, Zajac AJ, Miller JD, Slansky J, and Ahmed R. (1998). Counting antigen-specific CD8 T cells: a reevaluation of bystander activation during viral infection. Immunity 8, 177–187. 10.1016/s1074-7613(00)80470-7. [PubMed: 9491999]

26. Altman JD, Moss PA, Goulder PJ, Barouch DH, McHeyzer-Williams MG, Bell JI, McMichael AJ, and Davis MM (1996). Phenotypic analysis of antigen-specific T lyMPEChocytes. Science 274, 94–6. [PubMed: 8810254]

27. Kaech SM, Tan JT, Wherry EJ, Konieczny BT, Surh CD, and Ahmed R. (2003). Selective expression of the interleukin 7 receptor identifies effector CD8 T cells that give rise to long-lived memory cells. Nat Immunol 4, 1191–1198. [PubMed: 14625547]

28. Chung HK, McDonald B, and Kaech SM (2021). The architectural design of CD8+ T cell responses in acute and chronic infection: Parallel structures with divergent fates. J. Exp. Med 218, e20201730. 10.1084/jem.20201730.

29. Reith W, and Mach B. (2001). The bare lyMPEChocyte syndrome and the regulation of MHC expression. Annu. Rev. Immunol 19, 331–373. [PubMed: 11244040]

30. Plumlee CR, Sheridan BS, Cicek BB, and Lefrancois L. (2013). Environmental cues dictate the fate of individual CD8+ T cells responding to infection. Immunity 39, 347–356. 10.1016/j.immuni.2013.07.014. [PubMed: 23932571]

31. Tubo NJ., Fife BT., Pagan AJ., Kotov DI., Goldberg MF., and Jenkins MK. (2016). Most microbe-specific naive CD4(+) T cells produce memory cells during infection. Science 351, 511–514. 10.1126/science.aad0483. [PubMed: 26823430]

32. Foulds KE, Zenewicz LA, Shedlock DJ, Jiang J, Troy AE, and Shen H. (2002). Cutting edge: CD4 and CD8 T cells are intrinsically different in their proliferative responses. J. Immunol 168, 1528–1532. [PubMed: 11823476]

33. Homann D, Teyton L, and Oldstone MB (2001). Differential regulation of antiviral T-cell immunity results in stable CD8+ but declining CD4+ T-cell memory. Nat. Med 7, 913–9. [PubMed: 11479623]

34. Moon JJ, Chu HH, Hataye J, Pagan AJ, Pepper M, McLachlan JB, Zell T, and Jenkins MK (2009). Tracking epitope-specific T cells. Nat. Protoc 4, 565–581. [PubMed: 19373228]

35. Vollers SS, and Stern LJ (2008). Class II major histocompatibility complex tetramer staining: progress, problems, and prospects. Immunology 123, 305–313. [PubMed: 18251991]

36. Davis MM, Altman JD, and Newell EW (2011). Interrogating the repertoire: broadening the scope of peptide–MHC multimer analysis. Nat. Rev. Immunol 11, 551–558. 10.1038/nri3020. [PubMed: 21760610]

37. Andreatta M, Trolle T, Yan Z, Greenbaum JA, Peters B, and Nielsen M. (2018). An automated benchmarking platform for MHC class II binding prediction methods. Bioinformatics 34, 1522–1528. 10.1093/bioinformatics/btx820. [PubMed: 29281002]

38. Robertson JM, Jensen PE, and Evavold BD (2000). DO11.10 and OT-II T cells recognize a C-terminal ovalbumin 323–339 epitope. J. Immunol 164, 4706–4712. [PubMed: 10779776]

39. Marshall HD, Chandele A, Jung YW, Meng H, Poholek AC, Parish IA, Rutishauser R, Cui W, Kleinstein SH, Craft J, et al. (2011). Differential

expression of Ly6C and T-bet distinguish effector and memory Th1 CD4(+) cell properties during viral infection. Immunity 35, 633–646. 10.1016/j.immuni.2011.08.016. [PubMed: 22018471]

40. Mosmann TR, and Coffman RL (1989). TH1 and TH2 cells: different patterns of lymphokine secretion lead to different functional properties. Annu. Rev. Immunol 7, 145–173. [PubMed: 2523712]

41. Mackay CR (2000). Follicular homing T helper (Th) cells and the Th1/Th2 paradigm. J. Exp. Med 192, f31–f34. [PubMed: 11104811]

42. Mitsdoerffer M, Lee Y, Jäger A, Kim H-J, Korn T, Kolls JK, Cantor H, Bettelli E, and Kuchroo VK (2010). Proinflammatory T helper type 17 cells are effective B-cell helpers. Proc. Natl. Acad. Sci. U. S. A 107, 14292–14297. 10.1073/pnas.1009234107. [PubMed: 20660725]

43. Choi YS., Yang JA., Yusuf I., Johnston RJ., Greenbaum J., Peters B., and Crotty S. (2013). Bcl6 expressing follicular helper CD4 T cells are fate committed early and have the capacity to form memory. J. Immunol 190, 4014–4026. 10.4049/jimmunol.1202963. [PubMed: 23487426]

44. Ciucci T, Vacchio MS, Gao Y, Tomassoni Ardori F, Candia J, Mehta M, Zhao Y, Tran B, Pepper M, Tessarollo L, et al. (2019). The emergence and functional fitness of memory CD4(+) T cells require the transcription factor Thpok. Immunity 50, 91–105 e4. 10.1016/j.immuni.2018.12.019. [PubMed: 30638736]

45. Hale JS, Youngblood B, Latner DR, Mohammed AU, Ye L, Akondy RS, Wu T, Iyer SS, and Ahmed R. (2013). Distinct memory CD4+ T cells with commitment to T follicular helper- and T helper 1-cell lineages are generated after acute viral infection. Immunity 38, 805–817. 10.1016/j.immuni.2013.02.020. [PubMed: 23583644]

46. Johnston RJ, Poholek AC, DiToro D, Yusuf I, Eto D, Barnett B, Dent AL, Craft J, and Crotty S. (2009). Bcl6 and BliMPEC-1 are reciprocal and antagonistic regulators of T follicular helper cell differentiation. Science 325, 1006–1010. 1175870 [pii] 10.1126/science.1175870. [PubMed: 19608860]

47. Kunzli M, Schreiner D, Pereboom TC, Swarnalekha N, Litzler LC, Lotscher J, Ertuna YI, Roux J, Geier F, Jakob RP, et al. (2020). Long-lived

T follicular helper cells retain plasticity and help sustain humoral immunity. Sci Immunol 5, eaay5552. 10.1126/sciimmunol.aay5552.

48. Ballesteros-Tato A, Leon B, Graf BA, Moquin A, Adams PS, Lund FE, and Randall TD (2012). Interleukin-2 inhibits germinal center formation by limiting T follicular helper cell differentiation. Immunity 36, 847–856. 10.1016/j.immuni.2012.02.012. [PubMed: 22464171]

49. Krueger PD, Goldberg MF, Hong S-W, Osum KC, Langlois RA, Kotov DI, Dileepan T, and Jenkins MK (2021). Two sequential activation modules control the differentiation of protective T helper-1 (Th1) cells. Immunity 54, 687–701.e4. 10.1016/j.immuni.2021.03.006. [PubMed: 33773107]

50. Lonnberg T, Svensson V, James KR, Fernandez-Ruiz D, Sebina I, Montandon R, Soon MS, Fogg LG, Nair AS, Liligeto U, et al. (2017). Single-cell RNA-seq and Computational analysis using temporal mixture modelling resolves Th1/Tfh fate bifurcation in malaria. Sci. Immunol 2. 10.1126/sciimmunol.aal2192.

51. Soon MSF, Lee HJ, Engel JA, Straube J, Thomas BS, Pernold CPS, Clarke LS, Laohamonthonkul P, Haldar RN, Williams CG, et al. (2020). Transcriptome dynamics of CD4+ T cells during malaria maps gradual transit from effector to memory. Nat. Immunol 21, 1597–1610. 10.1038/s41590-020-0800-8. [PubMed: 33046889]

52. Linterman MA, Beaton L, Yu D, Ramiscal RR, Srivastava M, Hogan JJ, Verma NK, Smyth MJ, Rigby RJ, and Vinuesa CG (2010). IL-21 acts directly on B cells to regulate Bcl-6 expression and germinal center responses. J. Exp. Med 207, 353–363. 10.1084/jem.20091738. [PubMed: 20142429]

53. Iyer SS., Latner DR., Zilliox MJ., McCausland M., Akondy RS., Penaloza-Macmaster P., Hal JS., Ye L., Mohammed AU., Yamaguchi T., et al. . (2013). Identification of novel markers for mouse CD4(+) T follicular helper cells. Eur. J. Immunol 43, 3219–3232. 10.1002/eji.201343469. [PubMed: 24030473]

54. Breitfeld D, Ohl L, Kremmer E, Ellwart J, Sallusto F, Lipp M, and Forster R. (2000). Follicular B helper T cells express CXC chemokine receptor 5,

localize to B cell follicles, and support immunoglobulin production. J. Exp. Med 192, 1545–1552. 10.1084/jem.192.11.1545. [PubMed: 11104797]

55. Szabo SJ, Kim ST, Costa GL, Zhang X, Fathman CG, and Glimcher LH (2000). A novel transcription factor, T-bet, directs Th1 lineage commitment. Cell 100, 655–669. [PubMed: 10761931]

56. Ciucci T, Vacchio MS, Chen T, Nie J, Chopp LB, McGavern DB, Kelly MC, and Bosselut R. (2022). Dependence on Bcl6 and BliMPEC1 drive distinct differentiation of murine memory and follicular helper CD4+ T cells. J. Exp. Med 219, e20202343. 10.1084/jem.20202343.

57. Chevalier N, Jarrossay D, Ho E, Avery DT, Ma CS, Yu D, Sallusto F, Tangye SG, and Mackay CR (2011). CXCR5 expressing human central memory CD4 T cells and their relevance for humoral immune responses. J. Immunol 186, 5556–5568. jimmunol.1002828 [pii] 10.4049/jimmunol.1002828. [PubMed: 21471443]

58. Shulman Z, Gitlin AD, Targ S, Jankovic M, Pasqual G, Nussenzweig MC, and Victora GD (2013). T follicular helper cell dynamics in germinal centers. Science 341, 673–677. 10.1126/science.1241680. [PubMed: 23887872]

59. Shaw LA, Deng TZ, Omilusik KD, Takehara KK, Nguyen QP, and Goldrath AW (2022). Id3 expression identifies CD4+ memory Th1 cells. Proc. Natl. Acad. Sci. U. S. A 119, e2204254119. 10.1073/pnas.2204254119.

60. Hu Z, Blackman MA, Kaye KM, and Usherwood EJ (2015). Functional heterogeneity in the CD4+ T cell response to murine γ-herpesvirus 68. J. Immunol 194, 2746–2756. 10.4049/jimmunol.1401928. [PubMed: 25662997]

61. Andreatta M, Tjitropranoto A, Sherman Z, Kelly MC, Ciucci T, and Carmona SJ (2022). A CD4+ T cell reference map delineates subtype-specific adaptation during acute and chronic viral infections. eLife 11, e76339. 10.7554/eLife.76339.

62. Johnston RJ, Choi YS, Diamond JA, Yang JA, and Crotty S. (2012). STAT5 is a potent negative regulator of TFH cell differentiation. J. Exp. Med 209, 243–250. 10.1084/jem.20111174. [PubMed: 22271576]

63. Lin JX., Migone TS., Tsang M., Friedmann M., Weatherbee JA., Zhou L., Yamauchi A., Bloom ET., Mietz J., John S., et al. . (1995). The role of shared receptor motifs and common Stat proteins in the generation of cytokine pleiotropy and redundancy by IL-2, IL-4, IL-7, IL-13, and IL-15. Immunity 2, 331–339. [PubMed: 7719938]

64. Oestreich KJ, Mohn SE, and Weinmann AS (2012). Molecular mechanisms that control the expression and activity of Bcl-6 in TH1 cells to regulate flexibility with a TFH-like gene profile. Nat. Immunol 13, 405–411. 10.1038/ni.2242. [PubMed: 22406686]

65. Afkarian M, Sedy JR, Yang J, Jacobson NG, Cereb N, Yang SY, Murphy TL, and Murphy KM (2002). T-bet is a STAT1-induced regulator of IL-12R expression in naive CD4+ T cells. Nat. Immunol 3, 549–557. 10.1038/ni794. [PubMed: 12006974]

66. Mullen AC, High FA, Hutchins AS, Lee HW, Villarino AV, Livingston DM, Kung AL, Cereb N, Yao TP, Yang SY, et al. (2001). Role of T-bet in commitment of TH1 cells before IL-12-dependent selection. Science 292, 1907–1910. 10.1126/science.1059835. [PubMed: 11397944]

67. Schulz EG, Mariani L, Radbruch A, and Hofer T. (2009). Sequential polarization and imprinting of type 1 T helper lymphocytes by interferon-gamma and interleukin-12. Immunity 30, 673–683. 10.1016/j.immuni.2009.03.013. [PubMed: 19409816]

68. Leal JM, Huang JY, Kohli K, Stoltzfus C, Lyons-Cohen MR, Olin BE, Gale M, and Gerner MY (2021). Innate cell microenvironments in lymph nodes shape the generation of T cell responses during type I inflammation. Sci. Immunol 6, eabb9435. 10.1126/sciimmunol.abb9435.

69. Liu X, Yan X, Zhong B, Nurieva RI, Wang A, Wang X, Martin-Orozco N, Wang Y, Chang SH, Esplugues E, et al. (2012). Bcl6 expression specifies the T follicular helper cell program in vivo. J. Exp. Med 209, 1841–1852, S1–24. 10.1084/jem.20120219. [PubMed: 22987803]

70. Nurieva RI, Chung Y, Martinez GJ, Yang XO, Tanaka S, Matskevitch TD, Wang YH, and Dong C. (2009). Bcl6 mediates the development of T follicular helper cells. Science 325, 1001–1005. 10.1126/science.1176676. [PubMed: 19628815]

71. Eto D, Lao C, DiToro D, Barnett B, Escobar TC, Kageyama R, Yusuf I, and Crotty S. (2011). IL-21 and IL-6 are critical for different aspects of B cell immunity and redundantly induce optimal follicular helper CD4 T cell (Tfh) differentiation. PLoS One 6, e17739. 10.1371/journal.pone.0017739.

72. Choi YS, Kageyama R, Eto D, Escobar TC, Johnston RJ, Monticelli L, Lao C, and Crotty S. (2011). ICOS receptor instructs T follicular helper cell versus effector cell differentiation via induction of the transcriptional repressor Bcl6. Immunity 34, 932–946. S1074–7613(11)00185–3 [pii] 10.1016/j.immuni.2011.03.023. [PubMed: 21636296]

73. Xu H, Li X, Liu D, Li J, Zhang X, Chen X, Hou S, Peng L, Xu C, Liu W, et al. (2013). Follicular T-helper cell recruitment governed by bystander B cells and ICOS-driven motility. Nature 496, 523–527. 10.1038/nature12058. [PubMed: 23619696]

74. Sawant DV., Sehra S., Nguyen ET., Jadhav R., Englert K., Shinnakasu R., Hangoc G., Broxmeyer HE., Nakayama T., Perumal NB., et al. . (2012). Bcl6 controls the Th2 inflammatory activity of regulatory T cells by repressing Gata3 function. J. Immunol 189, 4759–4769. 10.4049/jimmunol.1201794. [PubMed: 23053511]

75. Choi J, Diao H, Faliti CE, Truong J, Rossi M, Belanger S, Yu B, Goldrath AW, Pipkin ME, and Crotty S. (2020). Bcl-6 is the nexus transcription factor of T follicular helper cells via repressor-of-repressor circuits. Nat. Immunol 21, 777–789. 10.1038/s41590-020-0706-5. [PubMed: 32572238]

76. Choi YS, Gullicksrud JA, Xing S, Zeng Z, Shan Q, Li F, Love PE, Peng W, Xue HH, and Crotty S. (2015). LEF-1 and TCF-1 orchestrate T(FH) differentiation by regulating differentiation circuits upstream of the transcriptional repressor Bcl6. Nat. Immunol 16, 980–990. 10.1038/ni.3226. [PubMed: 26214741]

77. Gullicksrud JA, Li F, Xing S, Zeng Z, Peng W, Badovinac VP, Harty JT, and Xue HH (2017). Differential requirements for Tcf1 long isoforms in CD8(+) and CD4(+) T cell responses to acute viral infection. J. Immunol 199, 911–919. 10.4049/jimmunol.1700595. [PubMed: 28652395]

78. Wu T, Shin HM, Moseman EA, Ji Y, Huang B, Harly C, Sen JM, Berg LJ, Gattinoni L, McGavern DB, et al. (2015). TCF1 Is required for the T follicular helper cell response to viral infection. Cell Rep. 12, 2099–2110. 10.1016/j.celrep.2015.08.049. [PubMed: 26365183]

79. Carpio VH, Opata MM, Montañez ME, Banerjee PP, Dent AL, and Stephens R. (2015). IFN-γ and IL-21 double producing T cells are Bcl6-Independent and survive into the memory phase in Plasmodium chabaudi infection. PLoS One 10, e0144654. 10.1371/journal.pone.0144654.

80. Eisenbarth SC, Baumjohann D, Craft J, Fazilleau N, Ma CS, Tangye SG, Vinuesa CG, and Linterman M. (2021). CD4+ T cells that help B cells – a proposal for uniform nomenclature. Trends Immunol. 42, 658–669. 10.1016/j.it.2021.06.003. [PubMed: 34244056]

81. Morita R, Schmitt N, Bentebibel SE, Ranganathan R, Bourdery L, Zurawski G, Foucat E, Dullaers M, Oh S, Sabzghabaei N, et al. (2011). Human blood CXCR5(+)CD4(+) T cells are counterparts of T follicular cells and contain specific subsets that differentially support antibody secretion. Immunity 34, 108–121. S1074–7613(10)00491–7 [pii] 10.1016/j.immuni.2010.12.012. [PubMed: 21215658]

82. Wingender G, and Kronenberg M. (2015). OMIP-030: Characterization of human T cell subsets via surface markers. Cytom. Part J. Int. Soc. Anal. Cytol 87, 1067–1069. 10.1002/cyto.a.22788.

83. Keck S, Schmaler M, Ganter S, Wyss L, Oberle S, Huseby ES, Zehn D, and King CG (2014). Antigen affinity and antigen dose exert distinct influences on CD4 T-cell differentiation. Proc Natl Acad Sci U A 111, 14852–14857. 10.1073/pnas.1403271111.

84. Krishnamoorthy V., Kannanganat S., Maienschein-Cline M., Cook SL., Chen J., Bahroos N., Sievert E., Corse E., Chong A., and Sciammas R. (2017). The IRF4 gene regulatory module functions as a read-write integrator to dynamically coordinate T helper cell fate. Immunity 47, 481–497 e7. 10.1016/j.immuni.2017.09.001. [PubMed: 28930660]

85. Künzli M, Reuther P, Pinschewer DD, and King CG (2021). Opposing effects of T cell receptor signal strength on CD4 T cells responding to acute versus chronic viral infection. eLife 10, e61869. 10.7554/eLife.61869.

86. Nayar R, Schutten E, Bautista B, Daniels K, Prince AL, Enos M, Brehm MA, Swain SL, Welsh RM, and Berg LJ (2014). Graded levels of IRF4 regulate CD8+ T cell differentiation and expansion, but not attrition, in response to acute virus infection. J Immunol 192, 5881–5893. 10.4049/jimmunol.1303187. [PubMed: 24835398]

87. Kim C, Wilson T, Fischer KF, and Williams MA (2013). Sustained interactions between T cell receptors and antigens promote the differentiation of CD4(+) memory T cells. Immunity 39, 508–520. 10.1016/j.immuni.2013.08.033. [PubMed: 24054329]

88. Snook JP, Kim C, and Williams MA (2018). TCR signal strength controls the differentiation of CD4(+) effector and memory T cells. Sci. Immunol 3. 10.1126/sciimmunol.aas9103.

89. Tubo NJ, Pagan AJ, Taylor JJ, Nelson RW, Linehan JL, Ertelt JM, Huseby ES, Way SS, and Jenkins MK (2013). Single naive CD4+ T cells from a diverse repertoire produce different effector cell types during infection. Cell 153, 785–796. 10.1016/j.cell.2013.04.007. [PubMed: 23663778]

90. DiToro D, Winstead CJ, Pham D, Witte S, Andargachew R, Singer JR, Wilson CG, Zindl CL, Luther RJ, Silberger DJ, et al. (2018). Differential IL-2 expression defines developmental fates of follicular versus nonfollicular helper T cells. Science 361. 10.1126/science.aao2933.

91. Leon B, Bradley JE, Lund FE, Randall TD, and Ballesteros-Tato A. (2014). FoxP3+ regulatory T cells promote influenza-specific Tfh responses by controlling IL-2 availability. Nat. Commun 5, 3495. 10.1038/ncomms4495. [PubMed: 24633065]

92. Li J, Lu E, Yi T, and Cyster JG (2016). EBI2 augments Tfh cell fate by promoting interaction with IL-2-quenching dendritic cells. Nature 533, 110–114. 10.1038/nature17947. [PubMed: 27147029]

93. Glatman Zaretsky A, Taylor JJ, King IL, Marshall FA, Mohrs M, and Pearce EJ (2009). T follicular helper cells differentiate from Th2 cells in response to helminth antigens. J. Exp. Med 206, 991–999. 10.1084/jem.20090303. [PubMed: 19380637]

94. Hondowicz BD., An D., Schenkel JM., Kim KS., Steach HR., Krishnamurty AT., Keitany GJ., Garza EN., Fraser KA., Moon JJ., et al. . (2016). Interleukin-2-dependent allergen- specific tissue-resident memory cells drive asthma. Immunity 44, 155–166. 10.1016/j.immuni.2015.11.004. [PubMed: 26750312]

95. Reinhardt RL, Liang HE, and Locksley RM (2009). Cytokine-secreting follicular T cells shape the antibody repertoire. Nat. Immunol 10, 385–393. 10.1038/ni.1715. [PubMed: 19252490]

96. Quinn JL, Kumar G, Agasing A, Ko RM, and Axtell RC (2018). Role of TFH cells in promoting T helper 17-induced neuroinflammation. Front. Immunol 9. https://www.frontiersin.org/articles/10.3389/fimmu.2018.00382

97. Kotov JA, Kotov DI, Linehan JL, Bardwell VJ, Gearhart MD, and Jenkins MK (2019). BCL6 corepressor contributes to Th17 cell formation by inhibiting Th17 fate suppressors. J. Exp. Med 216, 1450–1464. 10.1084/jem.20182376. [PubMed: 31053612]

98. Laurence A, Tato CM, Davidson TS, Kanno Y, Chen Z, Yao Z, Blank RB, Meylan F, Siegel R, Hennighausen L, et al. (2007). Interleukin-2 signaling via STAT5 constrains T helper 17 cell generation. Immunity 26, 371–381. S1074–7613(07)00176–8 [pii] 10.1016/j.immuni.2007.02.009. [PubMed: 17363300]

99. Tubo NJ, and Jenkins MK (2014). CD4+ T Cells: guardians of the phagosome. Clin. Microbiol. Rev 27, 200–213. 10.1128/CMR.00097-13. [PubMed: 24696433]

100. Sallin MA, Sakai S, Kauffman KD, Young HA, Zhu J, and Barber DL (2017). Th1 Differentiation Drives the Accumulation of Intravascular, Non-protective CD4 T Cells during Tuberculosis. Cell Rep. 18, 3091–3104. 10.1016/j.celrep.2017.03.007. [PubMed: 28355562]

101. Goldberg MF, Roeske EK, Ward LN, Pengo T, Dileepan T, Kotov DI, and Jenkins MK (2018). Salmonella persist in activated macrophages in T cell-sparse granulomas but are contained by surrounding CXCR3 ligand-positioned Th1 cells. Immunity 49, 1090–1102 e7. 10.1016/j.immuni.2018.10.009.

102. Moguche AO, Shafiani S, Clemons C, Larson RP, Dinh C, Higdon LE, Cambier CJ, Sissons JR, Gallegos AM, Fink PJ, et al. (2015). ICOS and Bcl6-dependent pathways maintain a CD4 T cell population with memory-like properties during tuberculosis. J. Exp. Med 212, 715–728. 10.1084/jem.20141518. [PubMed: 25918344]

103. Crawford A, Angelosanto JM, Kao C, Doering TA, Odorizzi PM, Barnett BE, and Wherry EJ (2014). Molecular and transcriptional basis of CD4(+) T cell dysfunction during chronic infection. Immunity 40, 289–302. 10.1016/j.immuni.2014.01.005. [PubMed: 24530057]

104. Fahey LM, Wilson EB, Elsaesser H, Fistonich CD, McGavern DB, and Brooks DG (2011). Viral persistence redirects CD4 T cell differentiation toward T follicular helper cells. J. Exp. Med 208, 987–999. 10.1084/jem.20101773. [PubMed: 21536743]

105. Hong S-W, Krueger PD, Osum KC, Dileepan T, Herman A, Mueller DL, and Jenkins MK. (2022). Immune tolerance of food is mediated by layers of CD4+ T cell dysfunction. Nature 607, 762–768. 10.1038/s41586-022-04916-6. [PubMed: 35794484]

106. Burton DR, Ahmed R, Barouch DH, Butera ST, Crotty S, Godzik A, Kaufmann DE, McElrath MJ, Nussenzweig MC, Pulendran B, et al. (2012). A Blueprint for HIV Vaccine Discovery. Cell Host Microbe 12, 396–407. 10.1016/j.chom.2012.09.008. [PubMed: 23084910]

107. Rivino L, Messi M, Jarrossay D, Lanzavecchia A, Sallusto F, and Geginat J. (2004). Chemokine receptor expression identifies pre–T helper (Th)1, pre–Th2, and nonpolarized cells among human CD4+ central memory T cells. J. Exp. Med 200, 725–735. 10.1084/jem.20040774. [PubMed: 15381728]

108. Beura LK, Fares-Frederickson NJ, Steinert EM, Scott MC, Thompson EA, Fraser KA, Schenkel JM, Vezys V, and Masopust D. (2019). CD4(+) resident memory T cells dominate immunosurveillance and orchestrate local recall responses. J. Exp. Med 216, 1214–1229. 10.1084/jem.20181365. [PubMed: 30923043]

109. Lee JY, Skon CN, Lee YJ, Oh S, Taylor JJ, Malhotra D, Jenkins MK, Rosenfeld MG, Hogquist KA, and Jameson SC (2015). The transcription

factor KLF2 restrains CD4(+) T follicular helper cell differentiation. Immunity 42, 252–264. 10.1016/j.immuni.2015.01.013. [PubMed: 25692701]

110. Son YM, Cheon IS, Wu Y, Li C, Wang Z, Gao X, Chen Y, Takahashi Y, Fu Y-X, Dent AL, et al. (2021). Tissue-resident CD4+ T helper cells assist the development of protective respiratory B and CD8+ T cell memory responses. Sci. Immunol 6, eabb6852. 10.1126/sciimmunol.abb6852.

111. Swarnalekha N, Schreiner D, Litzler LC, Iftikhar S, Kirchmeier D, Künzli M, Son YM, Sun J, Moreira EA, and King CG (2021). T resident helper cells promote humoral responses in the lung. Sci. Immunol 6, eabb6808. 10.1126/sciimmunol.abb6808.

112. Tan H-X, Esterbauer R, Vanderven HA, Juno JA, Kent SJ, and Wheatley AK (2019). Inducible bronchus-associated lymphoid tissues (iBALT) serve as sites of B cell selection and naturation following influenza infection in mice. Front. Immunol 10, 611. 10.3389/fimmu.2019.00611. [PubMed: 30984186]

113. Gregersen PK (1989). HLA class II polymorphism: implications for genetic susceptibility to autoimmune disease. Lab. Investig. J. Tech. Methods Pathol 61, 5–19.

114. Song S, Han M, Zhang H, Wang Y, and Jiang H. (2013). Full screening and accurate subtyping of HLA-A*02 alleles through group-specific amplification and mono-allelic sequencing. Cell. Mol. Immunol 10, 490–496. 10.1038/cmi.2013.33. [PubMed: 23954948]

115. Castelli FA., Buhot C., Sanson A., Zarour H., Pouvelle-Moratille S., Nonn C., Gahery-Ségard H., Guillet J-G., Ménez A., Georges B., et al. . (2002). HLA-DP4, the most frequent HLA II molecule, defines a new supertype of peptide-binding specificity. J. Immunol 169, 6928–6934. 10.4049/jimmunol.169.12.6928. [PubMed: 12471126]

116. Obar JJ, Molloy MJ, Jellison ER, Stoklasek TA, Zhang W, Usherwood EJ, and Lefrançois L. (2010). CD4+ T cell regulation of CD25 expression controls development of short-lived effector CD8+ T cells in primary and secondary responses. Proc. Natl. Acad. Sci. U. S. A 107, 193–198. 10.1073/pnas.0909945107. [PubMed: 19966302]

117. Cui W, Liu Y, Weinstein JS, Craft J, and Kaech SM (2011). An interleukin-21-interleukin-10-STAT3 pathway is critical for functional maturation of memory CD8+ T cells. Immunity 35, 792–805. 10.1016/j.immuni.2011.09.017. [PubMed: 22118527]

118. Tubo, N.J., and Jenkins, M.K. (2014). CD4+ T Cells: guardians of the phagosome. Clinical microbiology reviews *27*, 200–213. https://doi.org/10.1128/CMR.00097-13.

121. Kurtulus, S., Tripathi, P., Opferman, J.T., and Hildeman, D.A. (2010). Contracting the 'mus cells'—does down-sizing suit us for diving into the memory pool? Immunological reviews *236*, 54–67. https://doi.org/10.1111/j.1600-065X.2010.00920.x.

122. Milner, J.J., Toma, C., He, Z., Kurd, N.S., Nguyen, Q.P., McDonald, B., Quezada, L., Widjaja, C.E., Witherden, D.A., Crowl, J.T., et al. (2020). Heterogenous Populations of Tissue-Resident CD8+ T Cells Are Generated in Response to Infection and Malignancy. Immunity *52*, 808-824.e7. https://doi.org/10.1016/j.immuni.2020.04.007.

125. Zhu, X., and Zhu, J. (2020). CD4 T Helper Cell Subsets and Related Human Immunological Disorders. Int J Mol Sci *21*, 8011. https://doi.org/10.3390/ijms21218011.

126. Sallusto, F., Geginat, J., and Lanzavecchia, A. (2004). Central memory and effector memory T cell subsets: function, generation, and maintenance. Annu. Rev. Immunol. *22*, 745–763.

127. Kunzli, M., and Masopust, D. (2023). CD4+ T cell memory. Nat Immunol *24*, 903–914.https://doi.org/10.1038/s41590-023-01510-4.

128. Kondrack, R.M., Harbertson, J., Tan, J.T., McBreen, M.E., Surh, C.D., and Bradley, L.M. (2003). Interleukin 7 regulates the survival and generation of memory CD4 cells. J. Exp. Med. *198*, 1797–1806.

129. Purton, J.F., Tan, J.T., Rubinstein, M.P., Kim, D.M., Sprent, J., and Surh, C.D. (2007). Antiviral CD4+ memory T cells are IL-15 dependent. The Journal of experimental medicine *204*, 951–961.

130. Seddon, B., Tomlinson, P., and Zamoyska, R. (2003). Interleukin 7 and T cell receptor signals regulate homeostasis of CD4 memory cells. Nat. Immunol. *4*, 680–686.

131. Ertelt, J.M., Rowe, J.H., Johanns, T.M., Lai, J.C., McLachlan, J.B., and Way, S.S. (2009). Selective priming and expansion of antigen-specific Foxp3- CD4+ T cells during Listeria monocytogenes infection. Journal of immunology *182*, 3032–3038.

132. Rees, W., Bender, J., Teague, T.K., Kedl, R.M., Crawford, F., Marrack, P., and Kappler, J. (1999). An inverse relationship between T cell receptor affinity and antigen dose during CD4(+) T cell responses in vivo and in vitro. Proc. Natl. Acad. Sci. U S A *96*, 9781-6.

135. Shafiani, S., Dinh, C., Ertelt, J.M., Moguche, A.O., Siddiqui, I., Smigiel, K.S., Sharma, P., Campbell, D.J., Way, S.S., and Urdahl, K.B. (2013). Pathogen-Specific Treg Cells Expand Early during Mycobacterium tuberculosis Infection but Are Later Eliminated in Response to Interleukin-12. Immunity *38*, 1261–1270. https://doi.org/10.1016/j.immuni.2013.06.003.

143. Upadhyay, G. (2019). Emerging Role of Lymphocyte Antigen-6 Family of Genes in Cancer and Immune Cells. Front. Immunol. *10*. https://doi.org/10.3389/fimmu.2019.00819.

144. Epperson, T.K., Patel, K.D., McEver, R.P., and Cummings, R.D. (2000). Noncovalent association of P-selectin glycoprotein ligand-1 and minimal determinants for binding to P-selectin. J Biol Chem *275*, 7839–7853. https://doi.org/10.1074/jbc.275.11.7839.

145. Zander, R., Khatun, A., Kasmani, M.Y., Chen, Y., and Cui, W. (2022). Delineating the transcriptional landscape and clonal diversity of virus-specific CD4+ T cells during chronic viral infection. Elife *11*, e80079. https://doi.org/10.7554/eLife.80079.

146. Szabo, S.J., Kim, S.T., Costa, G.L., Zhang, X., Fathman, C.G., and Glimcher, L.H. (2000). A novel transcription factor, T-bet, directs Th1 lineage commitment. Cell *100*, 655–669.

146. Feng, H., Zhao, Z., Zhao, X., Bai, X., Fu, W., Zheng, L., Kang, B., Wang, X., Zhang, Z., and Dong, C. (2024). A novel memory-like Tfh cell

subset is precursor to effector Tfh cells in recall immune responses. J Exp Med *221*, e20221927. https://doi.org/10.1084/jem.20221927.

147. Way, S.S., Kollmann, T.R., Hajjar, A.M., and Wilson, C.B. (2003). Cutting edge: protective cell mediated immunity to Listeria monocytogenes in the absence of myeloid differentiation factor 88. J Immunol *171*, 533–537. https://doi.org/10.4049/jimmunol.171.2.533.

148. Kamran, P., Sereti, K.-I., Zhao, P., Ali, S.R., Weissman, I.L., and Ardehali, R. (2013). Parabiosis in mice: a detailed protocol. J Vis Exp, 50556. https://doi.org/10.3791/50556.

149. Geginat, G., Schenk, S., Skoberne, M., Goebel, W., and Hof, H. (2001). A novel approach of direct ex vivo epitope mapping identifies dominant and subdominant CD4 and CD8 T cell epitopes from Listeria monocytogenes. Journal of immunology *166*, 1877–1884.

150. Becht, E., McInnes, L., Healy, J., Dutertre, C.A., Kwok, I.W.H., Ng, L.G., Ginhoux, F., and Newell, E.W. (2018). Dimensionality reduction for visualizing single-cell data using UMAP. Nat Biotechnol. https://doi.org/10.1038/nbt.4314.

151. Gerdes, J., Schwab, U., Lemke, H., and Stein, H. (1983). Production of a mouse monoclonal antibody reactive with a human nuclear antigen associated with cell proliferation. Int J Cancer *31*, 13–20.

152. Guo, Y., Zhang, H., Xing, X., Wang, L., Zhang, J., Yan, L., Zheng, X., and Zhang, M. (2017). Gelsolin regulates proliferation, apoptosis and invasion in natural killer/T-cell lymphoma cells. Biol Open *7*, bio027557. https://doi.org/10.1242/bio.027557.

153. Makino, E., Sakaguchi, M., Iwatsuki, K., and Huh, N. (2004). Introduction of an N-terminal peptide of S100C/A11 into human cells induces apoptotic cell death. J Mol Med (Berl) *82*, 612–620. https://doi.org/10.1007/s00109-004-0560-1.

154. Liu, Y., Swiderski, C., Grimes, B., Wang, C., Liang, Y., and Van Zant, G. (2012). A Cell-Autonomous Myeloproliferative Phenotype Caused by Loss of Latexin in Stem and Progenitor Cells. Blood *120*, 2314. https://doi.org/10.1182/blood.V120.21.2314.2314.

155. Tachibana, I., Imoto, M., Adjei, P.N., Gores, G.J., Subramaniam, M., Spelsberg, T.C., and Urrutia, R. (1997). Overexpression of the TGFbeta-regulated zinc finger encoding gene, TIEG, induces apoptosis in pancreatic epithelial cells. J Clin Invest *99*, 2365–2374. https://doi.org/10.1172/JCI119418.

156. Flomerfelt, F.A., Briehl, M.M., Dowd, D.R., Dieken, E.S., and Miesfeld, R.L. (1993). Elevated glutathione S-transferase gene expression is an early event during steroid-induced lymphocyte apoptosis. J Cell Physiol *154*, 573–581. https://doi.org/10.1002/jcp.1041540316.

157. Porter, A.G., and Janicke, R.U. (1999). Emerging roles of caspase-3 in apoptosis. Cell Death Differ *6*, 99–104. https://doi.org/10.1038/sj.cdd.4400476.

158. Tsuchiya, K. (2020). Inflammasome-associated cell death: Pyroptosis, apoptosis, and physiological implications. Microbiology and Immunology *64*, 252–269. https://doi.org/10.1111/1348-0421.12771.

159. Chen, G., Sun, L., Han, J., Shi, S., Dai, Y., and Liu, W. (2019). RILPL2 regulates breast cancer proliferation, metastasis, and chemoresistance via the TUBB3/PTEN pathway. Am J Cancer Res *9*, 1583–1606.

160. Ishida, Y., Agata, Y., Shibahara, K., and Honjo, T. (1992). Induced expression of PD-1, a novel member of the immunoglobulin gene superfamily, upon programmed cell death. EMBO J *11*, 3887– 3895. https://doi.org/10.1002/j.1460-2075.1992.tb05481.x.

161. Sun, H., Hartigan, C.R., Chen, C.-W., Sun, Y., Tariq, M., Robertson, J.M., Krummey, S.M., Mehta, A.K., and Ford, M.L. (2021). TIGIT regulates apoptosis of risky memory T cell subsets implicated in belatacept-resistant rejection. Am J Transplant *21*, 3256–3267. https://doi.org/10.1111/ajt.16571.

162. Man, K., Gabriel, S.S., Liao, Y., Gloury, R., Preston, S., Henstridge, D.C., Pellegrini, M., Zehn, D., Berberich-Siebelt, F., Febbraio, M.A., et al. (2017). Transcription Factor IRF4 Promotes CD8+ T Cell Exhaustion and Limits the Development of Memory-like T Cells during Chronic Infection. Immunity *47*, 1129-1141.e5. https://doi.org/10.1016/j.immuni.2017.11.021.

163. Miyagawa, F., Zhang, H., Terunuma, A., Ozato, K., Tagaya, Y., and Katz, S.I. (2012). Interferon regulatory factor 8 integrates T-cell receptor and cytokine-signaling pathways and drives effector differentiation of CD8 T cells. Proc Natl Acad Sci U S A *109*, 12123–12128. https://doi.org/10.1073/pnas.1201453109.

164. Tsao, H.-W., Kaminski, J., Kurachi, M., Barnitz, R.A., DiIorio, M.A., LaFleur, M.W., Ise, W., Kurosaki, T., Wherry, E.J., Haining, W.N., et al. (2021). Batf-mediated Epigenetic Control of EffectorCD8+ T Cell Differentiation. Preprint at bioRxiv, ttps://doi.org/10.1101/2021.01.04.425241

165. Chao, D.T., and Korsmeyer, S.J. (1998). BCL-2 family: Regulators of cell death. Annual review of immunology *16*, 395–419.

166. Kumar, S., Ingle, H., Mishra, S., Mahla, R.S., Kumar, A., Kawai, T., Akira, S., Takaoka, A., Raut, A.A., and Kumar, H. (2015). IPS-1 differentially induces TRAIL, BCL2, BIRC3 and PRKCE in type I interferons-dependent and -independent anticancer activity. Cell Death Dis *6*, e1758–e1758. https://doi.org/10.1038/cddis.2015.122.

167. Feng, M., Liu, X., Hao, X., Ren, Y., Dong, G., Tian, J., Wang, Y., Du, L., Wang, Y., and Wang, C. (2023). Fatty Acids Support the Fitness and Functionality of Tumor-Resident CD8+ T Cells by Maintaining SCML4 Expression. Cancer Res *83*, 3368–3384. https://doi.org/10.1158/0008-5472.CAN- 23-0287.

168. Barbagallo, F., Rotilio, V., Assenza, M.R., Aguanno, S., Orsini, T., Putti, S., Isidori, A.M., Lenzi, A., Naro, F., De Angelis, L., et al. (2020). PDE2A Is Indispensable for Mouse Liver Development and Hematopoiesis. Int J Mol Sci *21*, 2902. https://doi.org/10.3390/ijms210829 02.

169. Wang, L., and Tsai, C.-C. (2008). Atrophin proteins: an overview of a new class of nuclear receptor corepressors. Nucl Recept Signal *6*, e009. https://doi.org/10.1621/nrs.06009.

170. Khan, O., Giles, J.R., McDonald, S., Manne, S., Ngiow, S.F., Patel, K.P., Werner, M.T., Huang, A.C., Alexander, K.A., Wu, J.E., et al. (2019). TOX transcriptionally and epigenetically programs CD8+ T cell exhaustion. Nature *571*, 211–218. https://doi.org/10.1038/s41586-019-1325-x.

171. Carpier, J.-M., Zucchetti, A.E., Bataille, L., Dogniaux, S., Shafaq-Zadah, M., Bardin, S., Lucchino, M., Maurin, M., Joannas, L.D., Magalhaes, J.G., et al. (2018). Rab6-dependent retrograde traffic of LAT controls immune synapse formation and T cell activation. J Exp Med *215*, 1245–1265. https://doi.org/10.1084/jem.20162042.

172. Woodring, T., Dewey, C.N., Santos Dias, L.D., He, X., Dobson, H.E., Wuthrich, M., and Klein, B. (2022). Distinctive populations of CD4+T cells associated with vaccine efficacy. iScience *25*, 104934. https://doi.org/10.1016/j.isci.2022.104934.

173. Kurelic, R., Krieg, P.F., Sonner, J.K., Bhaiyan, G., Ramos, G.C., Frantz, S., Friese, M.A., and Nikolaev, V.O. (2021). Upregulation of Phosphodiesterase 2A Augments T Cell Activation by Changing cGMPEC/cAMPEC Cross-Talk. Front Pharmacol *12*, 748798. https://doi.org/10.3389/fphar.2021.748798.

174. Burmeister, D.W., Smith, E.H., Cristel, R.T., McKay, S.D., Shi, H., Arthur, G.L., Davis, J.W., and Taylor, K.H. (2017). The expression of RUNDC3B is associated with promoter methylation in lymphoid malignancies. Hematol Oncol *35*, 25–33. https://doi.org/10.1002/hon.2238.

175. Ray, J.P., Staron, M.M., Shyer, J.A., Ho, P.C., Marshall, H.D., Gray, S.M., Laidlaw, B.J., Araki, K., Ahmed, R., Kaech, S.M., et al. (2015). The Interleukin-2-mTORc1 Kinase Axis Defines the Signaling, Differentiation, and Metabolism of T Helper 1 and Follicular B Helper T Cells. Immunity *43*, 690–702. https://doi.org/10.1016/j.immuni.2015.08.017.

177. Bromley, S.K., Akbaba, H., Mani, V., Mora-Buch, R., Chasse, A.Y., Sama, A., and Luster, A.D. (2020). CD49a Regulates Cutaneous Resident Memory CD8+ T Cell Persistence and Response. Cell Rep *32*, 108085. https://doi.org/10.1016/j.celrep.2020.108085.

178. von Werdt, D., Gungor, B., Barreto de Albuquerque, J., Gruber, T., Zysset, D., Kwong Chung, C.K.C., Correa-Ferreira, A., Berchtold, R., Page, N., Schenk, M., et al. (2023). Regulator of G-protein signaling 1 critically supports CD8+ TRM cell-mediated intestinal immunity. Front Immunol *14*, 1085895. https://doi.org/10.3389/fimmu.2023.1085895.

179. Carlson, C.M., Endrizzi, B.T., Wu, J., Ding, X., Weinreich, M.A., Walsh, E.R., Wani, M.A., Lingrel, J.B., Hogquist, K.A., and Jameson, S.C. (2006). Kruppel-like factor 2 regulates thymocyte and T-cell migration. Nature *442*, 299–302. https://doi.org/10.1038/nature04882.

181. Horiuchi, S., Wu, H., Liu, W.-C., Schmitt, N., Provot, J., Liu, Y., Bentebibel, S.-E., Albrecht, R.A., Schotsaert, M., Forst, C.V., et al. Tox2 is required for the maintenance of GC TFH cells and the generation of memory TFH cells. Sci Adv *7*, eabj1249. https://doi.org/10.1126/sciadv.abj1249.

184. Pais Ferreira, D., Silva, J.G., Wyss, T., Fuertes Marraco, S.A., Scarpellino, L., Charmoy, M., Maas, R., Siddiqui, I., Tang, L., Joyce, J.A., et al. (2020). Central memory CD8+ T cells derive from stem-like Tcf7hi effector cells in the absence of cytotoxic differentiation. Immunity *53*, 985-1000.e11. https://doi.org/10.1016/j.immuni.2020.09.005.

185. Hess Michelini, R., Doedens, A.L., Goldrath, A.W., and Hedrick, S.M. (2013). Differentiation of CD8 memory T cells depends on Foxo1. J Exp Med *210*, 1189–1200. https://doi.org/10.1084/jem.20130392.

186. Gautam, S., Fioravanti, J., Zhu, W., Le Gall, J.B., Brohawn, P., Lacey, N.E., Hu, J., Hocker, J.D., Hawk, N.V., Kapoor, V., et al. (2019). The transcription factor c-Myb regulates CD8+ T cell stemness and antitumor immunity. Nat Immunol *20*, 337–349. https://doi.org/10.1038/s41590-018-0311-z.

187. Waldmann, T.A., Waldmann, R., Lin, J.-X., and Leonard, W.J. (2022). The implications of IL-15 trans-presentation on the immune response. Adv Immunol *156*, 103–132. https://doi.org/10.1016/bs.ai.2022.09.002.

188. Miao, T., Symonds, A.L.J., Singh, R., Symonds, J.D., Ogbe, A., Omodho, B., Zhu, B., Li, S., and Wang, P. (2017). Egr2 and 3 control adaptive immune responses by temporally uncoupling expansion from T cell differentiation. Journal of Experimental Medicine *214*, 1787–1808. https://doi.org/10.1084/jem.20160553.

189. Hayward, A.R., Shriber, M., Cooke, A., and Waldmann, H. (1993). Prevention of Diabetes but not Insulitis in NOD Mice Injected with Antibody

to CD4. Journal of Autoimmunity *6*, 301–310. https://doi.org/10.1006/jaut.1993.1026.

191. Buchholz, V.R., Flossdorf, M., Hensel, I., Kretschmer, L., Weissbrich, B., Graf, P., Verschoor, A., Schiemann, M., Hofer, T., and Busch, D.H. (2013). Disparate individual fates compose robust CD8+ T cell immunity. Science *340*, 630–635. https://doi.org/10.1126/science.1235454.

192. Araki, K., Turner, A.P., Shaffer, V.O., Gangappa, S., Keller, S.A., Bachmann, M.F., Larsen, C.P., and Ahmed, R. (2009). mTOR regulates memory CD8 T-cell differentiation. Nature *460*, 108–112. https://doi.org/nature08155 [pii] 10.1038/nature08155.

193. Hu, Z., Blackman, M.A., Kaye, K.M., and Usherwood, E.J. (2015). Functional heterogeneity in the CD4+ T cell response to murine γ-herpesvirus 68. J Immunol *194*, 2746–2756. https://doi.org/10.4049/jimmunol.1401928.

194. Lopez-Yglesias, A.H., Burger, E., Araujo, A., Martin, A.T., and Yarovinsky, F. (2018). T-bet independent Th1 response induces intestinal immunopathology during Toxoplasma gondii infection. Mucosal Immunol *11*, 921–931. https://doi.org/10.1038/mi.2017.102.

195. Pritchard, G.H., Hall, A.O., Christian, D.A., Wagage, S., Fang, Q., Muallem, G., John, B., Zaretsky, A.G., Dunn, W.G., Perrigoue, J., et al. (2015). Diverse roles for T-bet in the effector responses required for resistance to infection. J Immunol *194*, 1131–1140. https://doi.org/10.4049/jimmunol.1401617.

196. Demoulin, J.B., and Renauld, J.C. (1998). Signaling by cytokines interacting with the interleukin- 2 receptor gamma chain. Cytokines Cell Mol Ther *4*, 243–256.

197. Schenkel, J.M., Fraser, K.A., Casey, K.A., Beura, L.K., Pauken, K.E., Vezys, V., and Masopust, D. (2016). IL-15-Independent Maintenance of Tissue-Resident and Boosted Effector Memory CD8 T Cells. J Immunol *196*, 3920–3926. https://doi.org/10.4049/jimmunol.1502337.

198. Kraus, M., Alimzhanov, M.B., Rajewsky, N., and Rajewsky, K. (2004). Survival of resting mature B lymphocytes depends on BCR signaling via the Igalpha/beta heterodimer. Cell *117*, 787–800.

199. Ernst, B., Lee, D.S., Chang, J.M., Sprent, J., and Surh, C.D. (1999). The peptide ligands mediating positive selection in the thymus control T cell survival and homeostatic proliferation in the periphery. Immunity *11*, 173–181.

200. Lee, Y., Siniscalco, E.R., Kraft, M., and Eisenbarth, S.C. (2023). Don't FRET-Antigens in the follicle are protected from degradation. Sci Immunol *8*, eadh3114. https://doi.org/10.1126/sciimmunol.adh3114.

201. J G Tew, G F Burton, L I Kupp, and A Szakal (1993). Follicular dendritic cells in germinal center reactions. Adv. Exp. Med. Biol. *329*, 461–465.

202. Heesters, B.A., Myers, R.C., and Carroll, M.C. (2014). Follicular dendritic cells: dynamic antigen libraries. Nat Rev Immunol *14*, 495–504. https://doi.org/10.1038/nri3689.

203. Martin, M.D., Kim, M.T., Shan, Q., Sompallae, R., Xue, H.-H., Harty, J.T., and Badovinac, V.P. (2015). Phenotypic and Functional Alterations in Circulating Memory CD8 T Cells with Time after Primary Infection. PLoS Pathog *11*, e1005219. https://doi.org/10.1371/journal.ppat.1005219.

204. Gattinoni, L., Speiser, D.E., Lichterfeld, M., and Bonini, C. (2017). T memory stem cells in health and disease. Nat Med *23*, 18–27. https://doi.org/10.1038/nm.4241.

205. Finotto, S., Neurath, M.F., Glickman, J.N., Qin, S., Lehr, H.A., Green, F.H.Y., Ackerman, K., Haley, K., Galle, P.R., Szabo, S.J., et al. (2002). Development of spontaneous airway changes consistent with human asthma in mice lacking T-bet. Science *295*, 336–338. https://doi.org/10.1126/science.1065544.

206. Liou, Y.-H., Wang, S.-W., Chang, C.-L., Huang, P.-L., Hou, M.-S., Lai, Y.-G., Lee, G.A., Jiang, S.-T., Tsai, C.-Y., and Liao, N.-S. (2014). Adipocyte IL-15 regulates local and systemic NK cell development. J Immunol *193*, 1747–1758. https://doi.org/10.4049/jimmunol.1400868.